

27 NOV. 1980

NLR TR 79017 U

~~Bibliotheek Metaalkunde
T.H. Delft, Rotterdamseweg 137~~

NATIONAAL LUCHT- EN RUIMTEVAARTLABORATORIUM

NATIONAL AEROSPACE LABORATORY NLR

THE NETHERLANDS

NLR TR 79017 U

Bibliotheek TU Delft
Faculteit der Luchtvaart- en Ruimtevaarttechni
Kluyverweg 1
2629 HS Delft

ENGINEERING PROPERTIES OF THE RECENTLY DEVELOPED ALUMINIUM ALLOY DESIGNATED 7010

BY

W.G.J. 'tHART AND L. SCHRA

Bibliotheek TU Delft
Faculteit der Luchtvaart- en Ruimtevaarttechniek
Kluyverweg 1
2629 HS Delft



Reprints from this publication may be made on condition that full credit be given to the Nationaal Lucht- en Ruimtevaartlaboratorium (National Aerospace Laboratory NLR) and the Author(s)

763926

DOCUMENT CONTROL SHEET

	ORIGINATOR'S REF. NLR TR 79017 U		SECURITY CLASS. Unclassified
ORIGINATOR	National Aerospace Laboratory NLR Amsterdam. The Netherlands		
TITLE	Engineering properties of the recently developed aluminium alloy designated 7010		
PRESENTED AT			
AUTHORS	W.G.J. 't Hart, L. Schra	DATE Febr. 1979	pp 53 ref 12
DESCRIPTORS	Aluminium alloys Tensile tests Mechanical properties Fatigue tests Fracture strength Corrosion tests Stress corrosion cracking Metal plates Materials tests Gust loads Toughness Thickness		
ABSTRACT	<p>An experimental investigation was performed on 80 mm thick plate material of 7010-T7651 and 7010-T73651 developed by Alcan Industries Ltd in U.K. The testing programme involved: tensile tests, fracture toughness, stress corrosion and fatigue tests. For comparison a similar investigation was carried out on 7075-T7351 Alcoa plate material.</p>		
<p>Bibliotheek TU Delft Fac. Lucht- en Ruimtevaart</p>  <p>c 3123895</p>			

NLR TR 79017 U

ENGINEERING PROPERTIES OF THE RECENTLY DEVELOPED
ALUMINIUM ALLOY DESIGNATED 7010

by

W.G.J. 't Hart and L. Schra

SUMMARY

Alcan Industries Ltd has developed an AlZnMgCu alloy, designated 7010, with high static strength and improved stress corrosion and fracture toughness properties in comparison with the 7075 alloy.

The National Aerospace Laboratory (NLR) performed an experimental investigation on 80 mm thick plate material of 7010-T7651 and 7010-T73651. The testing programme involved: tensile tests, fracture toughness, stress corrosion and fatigue tests.

For comparison a similar investigation was carried out on 7075-T7351 plate material.

This investigation has been performed under contract with the Netherlands Agency for Aerospace Programmes (NIVR), contractno. 1743.

Division: Structures and Materials

Prepared: WGJ'tH/LS/ *wjfl* *SB*

Approved: RJHW *W*

Completed : Febr. 1979

Ordernumber: 101.316

Typ. : AvdV

CONTENTS

	Page
1 INTRODUCTION	3
2 EXPERIMENTAL PROGRAMME	3
3 TENSILE TESTS	4
4 STRESS CORROSION INVESTIGATION	5
4.1 Stress corrosion crack initiation tests	5
4.1.1 Results	6
4.1.2 Outdoor exposure tests	7
4.2 Stress corrosion crack growth tests	7
4.2.1 Results	8
5 FRACTURE TOUGHNESS TESTS	9
5.1 CT fracture toughness	10
5.2 SENB fracture toughness	10
6 FATIGUE CRACK PROPAGATION TESTS	11
6.1 Testing procedure	11
6.2 Results of the fatigue tests	13
7 DISCUSSION	14
8 CONCLUSIONS	14
9 ACKNOWLEDGEMENTS	15
13 tables	
24 figures	
APPENDIX A ASTM REQUIREMENTS FOR FRACTURE TOUGHNESS TESTING	
(1 page)	
(53 pages in total)	

1 INTRODUCTION

The new high strength aluminium alloy 7010 has been developed by ALCAN Industries Ltd in the U.K. The alloy is produced as plate material, and heat treatments with the temper designations T7651 and T73651 are applied. Owing to reduced quench sensitivity the good corrosion properties are retained for thicker sections while also the mechanical properties are similar or superior to those of existing 7000 series alloys for equivalent heat treatments.

In the frame work of an international collaborative programme between the RAE, DFVLR, ONERA and NLR (Garteur 3 working group) the alloy 7010 is tested for stress corrosion properties and mechanical properties. ALCAN supplied plate material to the participants for investigation.

In this report the results of the NLR testing programme on 7010 are presented together with comparative results for 7075-T7351 plate.

2 EXPERIMENTAL PROGRAMME

ALCAN Industries Ltd supplied batches of the 7010 alloy to the NLR. The following batches were investigated

Batch No. 70 JH1 : 7010-T7651 size 80 x 500 x 880 mm*

Batch No.129 KH1 : 7010-T73651 size 80 x 500 x 880 mm

The specified chemical composition of 7010 is given in table 1a together with the composition limits of other alloys from the 7000 series.

Comparison of the composition limits presented in table 1a shows the Alcan alloy to be more or less equivalent to the Alcoa alloy 7050, except for the lower copper content. Particular attention is paid to controlling the iron and silicon impurities to low levels, thereby improving the fracture toughness of the material. Zirconium is added to reduce the quench sensitivity, i.e. to achieve good strength properties in thick sections.

*)

Underlined numbers indicate rolling direction

The heat treatment of 7010 involves a one-step ageing at a temperature of 442-445 K for both specifications. Only the ageing time is increased for T73651. (T7651 is aged 6 hours at 442-445 K and T73651 is aged 10 hours at 442-445 K).

At the NLR, the batches 70 JH1 and 129 KH1 were tested for corrosion and mechanical properties.

The testing programme consisted of

- tensile tests
- stress corrosion crack initiation tests
- stress corrosion crack growth tests
- fracture toughness tests
- fatigue crack growth tests

An almost similar investigation has been performed on 7075-T7351 Alcoa plate material (390 x 400 x 63 mm) received via DFVLR.

An outline of the testing programme is shown in tables 2a and 2b. A chemical element analysis of the tested materials is given in table 1b.

For microscopic investigation of the grain direction microsections have been prepared out of surface, centre and $\frac{1}{4}$ plate thickness material.

Three dimensional views of the local grain orientations are shown in figures 1 to 3. No evident influence of the location through the thickness on the grain orientation was observed.

3 TENSILE TESTS

Tensile specimens were machined from three locations (centre, $\frac{1}{4}t$, $\frac{3}{4}t$) through the thickness of the plate material in the longitudinal and transverse directions. The specimen dimensions are given in figure 4. Testing was executed in accordance with the ASTM specification E 8-69.

In table 3 the test results for 7010-T7651, 7010-T73651 and 7075-T7351 are compiled. No influence of the position through the plate thickness on the tensile strength was observed, nor was there a difference between longitudinal and long transverse strength. The obtained strength values agree well with those supplied by the

manufacturer (Ref.2) for the same batch. Comparison of the tensile strengths of 7010-T73651 and 7075-T7351 reveals no significant differences.

4 STRESS CORROSION INVESTIGATION

4.1 Stress corrosion crack initiation tests

For the stress corrosion crack initiation tests tuning-fork type specimens were used. The shape and dimensions of the specimens are sketched in figure 5. Five locations through the plate thickness were considered in this SCC investigation.

The specimens were prestressed to an equivalent maximum strain of 0.6 % by clamping them on closely dimensioned plastic strips. The screws used for clamping and the surrounded area of the specimens were sealed with wax to avoid dissimilar metal corrosion.

Corrosion tests were carried out in a paddle wheel (alternate immersion) and by continual immersion in a corrosive solution. The paddle wheel rotates with a speed of one revolution per hour during which the specimens are immersed in a corrosive solution for 10 minutes (Fig.6). Temperature and relative humidity were controlled at 20°C and 55 to 65 % RH, respectively.

The corrosive solutions used in this investigation were a 3½ % NaCl solution with pH 6-7 for the paddle wheel, and a corrosion solution according to the German specification LN65666. The latter specification involves continual immersion in a 2 % NaCl + 0.5 % Na₂CrO₄ solution with pH = 3. Sodium dichromate is added to diminish attack by pitting corrosion, which might obscure the appearance of stress corrosion cracks. The SCC specimens have to be pickled to ensure identical surface conditions after milling.

According to the specification LN65666 a maximum stress of $0.75 \times \sigma_{0.2}$ is prescribed. However, in the present investigation the SCC specimens were all loaded to a maximum strain of 0.6 %.

Inspection for stress corrosion crack initiation occurred daily using a binocular magnifying glass.

An overview of the performed SCC tests and the used environments is shown in table 4.

4.1.1 Results

Paddle wheel alternate immersion tests

None of the SCC specimens out of 7010-T7651, 7010-T73651 and 7075-T7351 failed during 1400 hours of testing. This means that the concerned alloys are highly resistant to stress corrosion cracking.

Corrosive attack was restricted to severe pitting corrosion, as shown in figures 7 and 8. Attack was more severe in the 7010 alloys than in the 7075-T7351 alloy. However, no evident difference in pit depths could be observed. Figures 9 and 10 show the cross sections of two SCC specimens with corrosion pits (depth ~ 0.5 mm). For the 7010-T73651 alloy transgranular cracks were observed starting from corrosion pits.

Transgranular cracking has been observed only in accelerated tests of highly stressed specimens that became severely pitted (Ref.3). Such cracking is not considered to be indicative of a service stress corrosion problem.

Continual immersion tests

One series of SCC tests started with exposure in a neutral 2 % NaCl + 0.5 % Na₂CrO₄ solution. To investigate the influence of the pickling treatment on SCC, half of the 7010-T7651 and 7010-T73651 specimens were not pickled.

After 1370 hours of testing none of the 7010 specimens had failed. Subsequently the pH of the solution was decreased to pH = 3 and the exposure was continued using the same specimens. After testing once again for 1400 hours, four 7010-T7651 and three 7010-T73651 specimens had failed. The stress corrosion lives are given in table 5. It is noteworthy that the failed specimens were unpickled.

In a second series, 7010 and 7075 specimens were exposed at once in the (2 % NaCl + 0.5 % Na₂CrO₄) solution with pH = 3. Also this time, half of the specimens were pickled. After 1670 hours of testing only one 7010-T7651 specimen showed an indication of a stress corrosion crack (a pickled specimen). No attack by general corrosion occurred during the continued immersion tests.

On account of the performed stress corrosion tests it can be concluded that the stress corrosion resistance of both 7010-T7651 and 7010-T73651 is very high.

4.1.2 Outdoor exposure tests

To investigate stress corrosion crack initiation under atmospheric conditions, tuning fork specimen were exposed outdoors. The specimen type and the stress condition were similar as used in laboratory tests. Outdoor exposure started in February 1978. After 1 year of exposure none of the 7010-T7651, 7010-T73651 and 7075-T7351 specimens was failed.

4.2 Stress corrosion crack growth tests

Double cantilever beam (DCB) type specimens were used to examine the stress corrosion crack growth. The shape and dimensions of this specimen type are shown in figure 11. Side grooves were applied to direct the crack along the midplane of the specimen.

To investigate stress corrosion crack growth the DCB specimen is preloaded with a bolt (constant displacement). The crack extension is measured periodically on the side surface of the specimen. The bottom of the side groove was rounded and polished to enable visual observation of the crack length.

The stress corrosion crack growth rate is governed by the stress intensity factor K . For the DCB type specimens K is defined by:

$$K = P \left[\frac{E}{2B_n} \cdot \frac{dC}{da} \right]^{\frac{1}{2}} \quad (\text{Ref.4}) \quad (4.2-1)$$

where K = stress intensity factor

P = applied load

B_n = net specimen thickness

E = Young's modulus

a = crack length

C = specimen compliance (ratio of displacement and load)

The dimensionless form of (eq. 4.2-1) can be written as

$$\frac{K\sqrt{H}}{E.v} = \frac{1}{E.C} \left[\frac{EH}{2B_n} \cdot \frac{dC}{da} \right]^{\frac{1}{2}} \quad (4.2-2)$$

where H = half of the specimen height

v = displacement

After the determination of a compliance calibration for this specimen type a K calibration curve as a function of the crack length could be plotted, figure 12 (Ref.5). This figure shows that at a constant deflection K decreases with increasing crack length. During stress corrosion crack growth K decreases to a threshold value, called K_{ISCC} , below which no significant crack growth* occurs. Initially the stress intensity factor for mechanical instability for this specimen type was determined to provide a guide for the magnitude of the initial K-factor to be applied in the SCC test. A mechanical crack as well as a fatigue crack as starter notch were applied. The K_C results are presented in table 6. It appeared that the K_C values for fatigue precracked specimens were lower than those for mechanically precracked specimens.

Based on these K_C tests, an initial stress intensity of $17 \text{ MPa m}^{\frac{1}{2}}$ and $21 \text{ MPa m}^{\frac{1}{2}}$ was chosen for 7010-T7651 and 7010-T73651, respectively. Two initial crack lengths have been considered in the crack growth investigation i.e. 25 mm and 40 mm. The specimens were all fatigue precracked.

The DCB specimens were exposed to two different corrosive environments:

- i Moistening twice every working day with a $3\frac{1}{2}$ % NaCl solution pH = 6-7., spouted from a siphon (temperature 21°C ; $55\% < \text{RH} < 65\%$)
- ii Continual immersion in a (2 % NaCl + 0.5 % Na_2CrO_4) solution pH = 3 according to LN65666.

Inspection of the specimens was executed about once a week for 6 months.

4.2.1 Results

The results of the crack growth measurements are compiled in table 7. Slight crack growth was observed for the specimens exposed to NaCl moistening in the open air. Specimens of 7010-T7651 showed a larger crack growth than specimens of 7010-T73651.

The stress corrosion crack growth rate and the related stress intensity factors have been calculated for the test periods 0 - 100

*) crack growth rate $< 10^{-7} \text{ mm/s}$

day's and 100 - 196 day's. The values are plotted in figure 13 together with the results of ALCAN Industries. It is seen that the NLR results fall reasonably within the crack growth rate range indicated by ALCAN. However, the crack growth tendency of the 7010-T7651 specimens does not show the expected decrease in crack growth rate for lower stress intensity factors. Probably there is a different driving force for crack extension that obscures the results of the DCB tests.

Hyatt (Ref.6) and Dorward (Ref.7) reported that the build up of corrosion products in the crack of a DCB specimen can cause additional stresses at the crack tip. The stress intensity factor can reach a higher value than the stress intensity factor applied by external loading. This prevents the crack growth rate becoming smaller at nominally lower stress intensity factors.

Unloading of the tested DCB specimens revealed that the initially applied deflection did not diminish to zero. About 40 to 60 percent of the initial displacement was left. Therefore it can be assumed that corrosion - product wedging has influenced the crack growth rate.

The stress corrosion tests in the LN65666 solution resulted in negligible crack growth. When after the tests the bolts were removed the deflection decreased nearly completely to the deflection before loading indicating that no corrosion products were formed at the crack surfaces.

All the specimens have been broken mechanically to examine the fracture surfaces. It appeared that the real mean crack extension measured from the fracture surface was larger than was observed from the side grooves in the specimens, table 8. This was essentially caused by a rounded crack front.

5 FRACTURE TOUGHNESS TESTS

Fracture toughness tests have been performed on Single Edge Notch Bend (SENB) specimens and on Compact Tension (CT) specimens. The testing directions are indicated in table 2 and the specimen dimensions in figure 14 and 15. Testing and interpretation of the results were conducted according to the ASTM recommendations E 399-74.

5.1 CT fracture toughness

The specimens were fatigue precracked in a 20 kN Amsler Vibrophore. During fatigue cracking the maximum stress intensity did not exceed 60 % of the plane strain fracture toughness value determined in the subsequent test.

Testing was executed in a 200 kN hydraulic testing machine while the clip gauge output was recorded as a function of the load. A second line with 5 % offset to the linear part of the load displacement record was drawn to determine the load P_Q which serves as a basis to calculate a candidate fracture toughness K_Q .

$$K_Q = \frac{P_Q}{BW^{\frac{3}{2}}} \cdot f\left(\frac{a}{W}\right) \quad (\text{Ref.8}) \quad (5.1-1)$$

where:

P_Q = load at the intersection of the 5 % offset line and the load-displacement curve

B = specimen thickness

W = specimen width

$f\left(\frac{a}{W}\right)$ = a function, represented by a power series which is given in reference 8.

Further, there are different requirements to be met before K_Q can be called a valid plane strain fracture toughness, K_{Ic} . Appendix A gives a number of criteria to be fulfilled to obtain a valid K_{Ic} . The mentioned criteria are hardly influenced by the test procedure. Table 9a gives the compact tension test results and the calculated K_Q values. In the last column those validity criteria from appendix A are indicated which have not been fulfilled. The K_Q values are plotted in figure 16. The fracture toughness values measured by ALCAN (Ref.2) are indicated in the same figure. The crack extension of the LS orientation specimens strongly deviated from the S direction as shown in figure 17. Since no valid values were obtained, the K_Q values for the LS orientation are not plotted in figure 16.

5.2 SENB fracture toughness

The SENB specimen were fatigue precracked in a 20 kN Amsler Vibrophore. Testing and interpretation of the results were conducted

to the ASTM recommendations.

Load-displacement curves were recorded on a X-Y plotter and P_Q loads could be determined in the same way as described for the CT specimens.

The candidate fracture toughness for SENB tests was calculated according to:

$$K_Q = \frac{P_Q S}{BW^2} \cdot f\left(\frac{a}{W}\right) \quad (5.2-1)$$

where

S = span (160 mm)

$f\left(\frac{a}{W}\right)$ = a function, represented by a power series specific for the compact tension specimen (Ref.8)

B = specimen thickness

W = specimen width

Only a small number of bend specimens were tested, table 9b. The main purpose was to examine whether the SENB tests resulted in similar fracture toughness values as obtained with CT-tests. Schra (Ref.9) reported that for forging materials lower fracture toughness values were obtained for CT tests than for SENB tests (similar test directions). However, for the tested 7010 material no significant difference in K_{Ic} was observed. The results of 7075-T7351 could not be compared because all but one result was invalid.

6 FATIGUE CRACK PROPAGATION TESTS

6.1 Testing procedure

In the performed fatigue investigation, a standardized load spectrum, developed for flight simulation tests on transport aircraft wing structures, was used. The spectrum was taken as the median of the scatter band of gust load spectra for different transport aircraft and may be considered as representative for the load history of the wing root of a transport aircraft. This standardized spectrum was jointly developed by the Laboratorium für Betriebsfestigkeit (LBF), Darmstadt, Germany and the National Aerospace Laboratory (NLR) and is described

in reference 10.

The standardized load sequence based on this spectrum consists of 40.000 flights which were divided into 10 equal blocks of 4.000 flights. The averaged gust load spectrum, presented in figure 18 was approximated to by a stepped function, consisting of 10 load levels. The gust load spectrum was distributed over 10 different types of flight (A-J), each characterized by its own spectrum, varying from "good weather" to "storm" conditions. Examples of different flight types are shown in figure 19. The sequence of the flights was randomly selected by a computer with the exception of the very severe flights. The latter may have a predominant effect on the fatigue life and it was considered undesirable that the severe flights should have a chance to cluster together. The distribution of the most severe flights over the total block of 4.000 flights is given in table 10. An overview of the different types of flight and the number of load cycles within each flight is given in table 11.

In the ground-to-air cycle (GTAC) taxiing loads were not applied because these loads do not affect the fatigue life if they occur in compression (Ref.11). However, taxiing loads do increase the stress range of the GTAC, thus making this cycle more damaging. For that reason the minimum stress of the GTAC was chosen at a fairly severe level, namely $S_{a,min} = -0.5 S_{m,flight}$.

The amplitudes were truncated to the level of $S_{a,max} = 1.30 S_{m,flight}$.

Centre notched fatigue specimens, figure 20, were tested until complete failure. Four thicknesses have been tested i.e. 2, 5, 10 and 15 mm* in order to investigate the influence of material thickness on fatigue crack growth. To establish a possible influence of the location through the plate thickness on fatigue properties, core material as well as surface material was tested.

The specimens were fatigue precracked under constant amplitude loading in a 50 kN Vibrophore until a semi crack length of about 7 mm. Flight by flight loading was performed in a closed loop controlled electro hydraulic testing machine, made by the MTS division of Research Incorporated, with a maximum dynamic load capacity of 230 kN.

*) For 7075-T7351 only 5, 10 and 15 mm

The test frequency for the lower amplitudes was 15 cps. For the higher amplitudes the frequency was reduced in inverse proportion to the amplitude in view of the pumping and valve capacity of the fatigue machine.

The mean stress level for the fatigue tests was 55 MPa. Fatigue crack growth was measured continuously with an electric potential method, except for the 15 mm thick specimens. For the latter, crack growth was measured by visual observation of the fatigue crack. The number of flights at which the crack crossed reference lines that were inscribed on the specimen surface were noted.

6.2 Results of the fatigue tests

The fatigue lives of the tested specimens have been compiled in table 12. However, since the initial crack lengths of the specimens were not exactly similar, a better comparison could be made by considering the number of flights it takes the crack to grow from 10 to 20 mm (semi crack length), table 13.

No systematic difference in fatigue behaviour between core material and surface material was observed. But there is an evident thickness effect on the fatigue crack growth, as has been observed elsewhere (Ref.12). In figures 21 to 23 the semi crack lengths as a function of the number of flights are given for different material thicknesses. Continuous lines are plotted while small retardation effects after heavy flights are not indicated. The thickness effect is most pronounced for small thicknesses. In figure 24 the number of flights for 10 mm crack growth are plotted for the tested thicknesses. It is shown that the fatigue properties of 7075-T7351 are somewhat better than those of 7010-T73651. Further the higher strength properties of 7010-T7651 are connected with lower fatigue properties.

The fatigue tests did show that the effect of specimen thickness on fatigue was most pronounced for small thicknesses. This indicates the crack growth under plane stress to be dominant for small thicknesses while the plane stress crack growth in the surface regions of thicker specimens has less influence on the over-all crack growth.

7 DISCUSSION

Stress corrosion initiation and stress corrosion crack growth tests have shown that the resistance to stress corrosion of the aluminium alloy 7010 is excellent for the T73651 as well as for the T7651 heat treatment. The stress corrosion initiation tests were performed at a stress level of about 420 MPa in different corrosive solutions. Almost all the specimens survived 1400 hours of testing.

The benefit of the German LN 65666 solution (continual immersion) for stress corrosion testing could not be evaluated by testing the highly resistant 7010 alloy. This should be investigated on more susceptible alloys.

From the stress corrosion crack growth tests it appeared that corrosion product wedging, in the case of moistening with a NaCl solution, obscured the real crack growth properties. Although the measured crack growth rate was already low it has to be considered as a conservative value.

Comparison of the engineering properties of 7075-T7351 and 7010-T73651 revealed that in general 7075-T7351 was slightly superior. A chemical analysis of the 7075 alloy pointed out that the tested plate material was a special quality 7075 alloy with a very low percentage of impurities table 1b. For this reason the obtained properties are close to the specifications for 7475-T7351.

The comparative investigation between 7010 plate material and different plate materials will be continued in 1979. A similar investigation as performed on 7010 will be carried out on 7050-T73651 plate material.

8 CONCLUSIONS

On account of the performed experimental investigation on 7010-T7651, 7010-T73651 and 7075-T7351 the following conclusions can be drawn.

1. The tensile properties of 7010-T7651 and 7010-T73651 fulfil the requirements for DTD 5120 and DTD 5130 respectively as specified in reference 1.

2. The fracture toughness properties of 7010 amply exceeded the required minimum values (Ref.1). There was a relatively small difference between the fracture toughness in the L-T and T-L direction. This can probably be related to the production of the plate material (cross rolling can reduce the orientation dependency of the fracture toughness).
3. Stress corrosion crack initiation tests revealed that 7010 in the T7651 and T73651 tempers is resistant to stress corrosion cracking.
4. The stress corrosion crack growth rate of 7010-T7651 under NaCl moistening is very low, $\approx 10^{-7}$ mm/s at $K = 17 \text{ MPa m}^{\frac{1}{2}}$. Owing to corrosion-product wedging this value is even conservative. The crack growth of 7010-T73651 was still smaller.
5. Fatigue tests under flight simulation loading have shown that the material location through the plate thickness did not influence the fatigue behaviour of the 7010 and 7075 alloy.
6. Fatigue testing of 2, 5, 10 and 15 mm thick specimens revealed a thickness effect which was most pronounced for the small thicknesses. The fatigue life decreased with increasing specimen thickness.
7. The overall properties were somewhat better for 7075-T7351 than for 7010-T73651. This can be attributed to the low percentage of impurities in 7075-T7351 that resulted in a special quality 7075-T7351 plate material.

9

ACKNOWLEDGEMENTS

The experiments were carried out by H.J. de Jager, J.H. Nassette P.J. Tromp and K.A. v.d. Sijde.

10 REFERENCES

1. Reynolds M.A.,
Fitzsimmons P.E. and
Harris J.G. Presentation of properties of a new
high strength aluminium alloy
designated 7010,
28 September 1976.
2. Fitzsimmons P.E. Batch properties of 7010 plate,
Data presented in letters to the NLR
on 17, February 1977 and 21, March
1977.
3. Sprowls D.O. et al Evaluation of a proposed standard
method of testing for susceptibility
to stress corrosion cracking of high
strength 7xxx series aluminium alloy
products,
ASTM STP 610.
4. Gallagher J.P. Experimentally determined stress
intensity factors for several
contoured double cantilever beam
specimens,
Eng. Fracture Mech., Vol. 3, 1971.
5. Schra L. and Heat treatment studies of aluminium
van Leeuwen H.P. alloy forgings of the AZ 74.61 type,
NLR TR 74151 U, 1974.
6. Hyatt M.V. and Stress corrosion cracking of high
Speidel M.O. strength aluminium alloys,
Advances in corrosion science and
technology, Vol. 2 ed. by Fontana M.G.
and Staehle R.W., 1971.

7. Dorward R.C.,
Hasse K.R. and
Helfrich W.J.

Marine atmospheric corrosion tests on precracked specimens from high-strength aluminium alloys: Effect of corrosion-product wedging,
J. of Testing and Evaluation, Vol.6,
No. 4 July 1978.
8. Brown W.F. and
Strawley J.E.

Plane strain crack toughness testing of high strength metallic materials,
ASTM STP 410, 1967.
9. Schra L. and
van Leeuwen H.P.

Heat treatment studies of aluminium alloy forgings of the AZ 74.61 Type
Interim report No. 2: The effect of heat treatment on a variety of engineering properties,
NLR TR 74151, 1974
10. De Jonge J.B.,
Schütz D.,
Lowak H. and
Schijve J.

A standardized load sequence for flight simulation tests on transport aircraft wing structures,
LBF-Bericht FB-106, NLR TR 73029
March 1973.
11. Schijve J.

The accumulation of fatigue damage in aircraft materials and structures,
AGARDograph No. 157, 1972.
12. Wanhill R.J.H.

The effect of sheet thickness on flight simulation fatigue crack propagation in 2024-T3, 7475-T761 and mill annealed Ti-6Al-4V,
NLR MP 77024, July 1977.

TABLE 1a
Chemical compositions

Element	According to specification, %					
	7475	7079	7075	7175	7050	7010
Zn	5.2-6.2	3.8-4.8	5.1-6.1	5.1-6.1	5.7-6.7	5.7-6.7
Mg	1.9-2.6	2.9-3.7	2.1-2.9	2.1-2.9	1.9-2.6	2.2-2.7
Mn	0.06	0.1-0.3	0.3 max	0.10 max	0.10 max	0.30 max
Cu	1.2-1.9	0.4-0.8	1.2-2.0	1.2-2	2.0-2.6	1.5-2.0
Cr	0.18-0.25	0.10-0.25	0.18-0.40	0.18-0.30	0.04 max	0.05 max
Si	0.10	0.3 max	0.5 max		0.12 max	0.10 max
Fe	0.12	0.4 max	0.7 max	0.20 max	0.15 max	0.15 max
Ti	0.06	0.1 max	0.2 max	0.1 max	0.06 max	0.05 max
Zr	-	-	-	-	0.08-0.15	0.11-0.17
others each		0.05 max	0.05 max	0.05 max	0.05 max	
others total		0.15 max	0.15 max	0.15 max	0.15 max	

TABLE 1b
Chemical analysis of the tested materials

Element	7010 mean cast composition 3G718 1X166	7010 *	7075 *
Zn	6.13	6.45	6.24
Mg	2.31	2.36	2.46
Mn	< 0.01	< 0.005	< 0.005
Cu	1.72	1.72	1.66
Cr	< 0.01	< 0.05	0.20
Si	0.06	0.08	0.08
Fe	0.08	0.18	0.12
Ti	0.04	≤ 0.05	≤ 0.12
Zr	0.12	0.11	< 0.01

* determined by Wilton-Fijenoord B.V.

TABLE 2a

Testing programme for 7010 plate material

Properties	Specimen type and testing direction
Tensile properties	L and T direction
Stress corrosion crack initiation	Tuning fork type specimens (SL) tested by alternate immersion, continual immersion and outdoor exposure
Stress corrosion crack growth	Double cantilever beam specimen(SL)
Fracture toughness	Compact tension: LT;TL;LS;SL;TS;ST. Single edge cracked bend specimen: TS
Fatigue crack growth tests under flight simulation loading	Centre cracked specimen (LT) thickness: 15, 10, 5 and 2 mm

TABLE 2b

Testing programme for 7075 plate material

Properties	Specimen type and testing direction
Tensile properties	L and T direction
Stress corrosion crack initiation	Tuning fork type specimens tested by alternate immersion and continual immersion
Fracture toughness	Compact tension: LT;TL;LS;SL;TS;ST. Single edge cracked bend specimens: TS
Fatigue crack growth tests under flight simulation loading	Centre cracked specimen thickness: 15, 10 and 5 mm

TABLE 3
Strength properties of 7010 and 7075 plate material

Material	Location	$\sigma_{0.2}$ MPa		σ_{ult} MPa		δ %	
		L	T	L	T	L	T
70 JH1 7010-T7651	surface	477	477	517	536	12.2	11.2
	surface	473	467	516	531	12.2	10.4
	$\frac{1}{4}t$	471	475	519	522	11.2	9.8
	$\frac{1}{4}t$	474	462	525	525	10.6	10.4
	core	474	461	528	521	10.2	9.6
	mean	474	469	521	527	11.3	10.3
129 KH1 7010-T73651	surface	433	437	495	507	13.8	11.2
	surface	441	441	497	509	13.6	11.6
	$\frac{1}{4}t$	433	424	496	499	11.6	9.8
	$\frac{1}{4}t$	437	430	502	497	12.0	10.2
	core	436	426	498	496	11.4	10.6
	mean	436	432	498	502	12.5	10.7
7075-T7351	surface	434	441	504	516	13.2	12.2
	surface	433	429	502	507	14.0	12.0
	$\frac{1}{4}t$	421	421	495	498	11.6	11.8
	$\frac{1}{4}t$	427	419	498	497	12.0	11.8
	core	432	432	503	500	11.8	12.2
	mean	429	427	501	504	12.5	12.0

TABLE 4

Test programme for stress corrosion crack initiation

Material	Test method	Environment	Pretreatment	Number of tested specimens	Number of failed spec.
7010-T7651	A.I. paddle wheel	3½% NaCl, pH6-7	none	25	-
7010-T73651	A.I. paddle wheel	3½% NaCl, pH6-7	none	25	-
7075-T7351	A.I. paddle wheel	3½% NaCl, pH6-7	none	15	-
7010-T7651	C.I.	2% NaCl+0.5% Na ₂ CrO ₄ , pH7 + 1400 hours, pH3	none	15	- 4
7010-T7351	C.I.	2% NaCl+0.5% Na ₂ CrO ₄ , pH7 + 1400 hours, pH3	none	15	- 3
7010-T7651	C.I.	,,	pickled**	15	-
7010-T73651	C.I.	,,	pickled	15	-
7010-T7651	C.I.	2% NaCl+0.5% Na ₂ CrO ₄ , pH3	none	8	-
7010-T7651	C.I.	,,	pickled	8	1
7010-T73651	C.I.	,,	none	8	-
7010-T73651	C.I.	,,	pickled	8	-
7075-T7351	C.I.	,,	pickled	15	-

* Tuning fork type specimens
loaded to $\epsilon_{\max} \sim 0.6\%$

** pickling was executed according
to specification LN65666

A.I. Alternate immersion

C.I. Continual immersion

TABLE 5
Stress corrosion crack initiation lives of
failed specimens (all unpickled)

Material	Environment	Crack initiation life* (hours)
7010-T7651	continual immersion 2 % NaCl + 0.5 % Na ₂ CrO ₄ , pH3	382
		506
		506
		945
7010-T73651	continual immersion 2 % NaCl + 0.5 % Na ₂ CrO ₄ , pH3	315
		336
		1317

* The specimens survived already an exposure period of 1370 hours
in the corrosive solution: 2 % NaCl + 0.5 % Na₂CrO₄, pH7

TABLE 6
Stress intensity for mechanically instability

material	specimen nr.	K_c^* MPa $m^{1/2}$	K_c^{**} MPa $m^{1/2}$	K_c^{***} MPa $m^{1/2}$
7010-T7651	A1.7	27.2	21.8	20.2
	A1.8	26.9	19.5	18.9
	A2.7	29.6	-	
	A2.8	31.2	-	
	A3.7	26.3	19.8	19.1
	A3.8	26.0	20.7	20.4
7010-T73651	B1.7	31.9	-	
	B1.8	29.3	-	
	B2.7	33.7		
	B2.8	32.0	-	
	B3.7	29.0	24.9	23.4
	B3.8	30.4	24.1	23.7

* mean K_c of three measurements starting with a mechanical crack

** K_c determined after fatigue precracking

*** K_c based on the crack length determined in the centre of the fracture surface after forced breaking of the DCB specimen

TABLE 7

Stress corrosion crack growth of 7010-TT651 and 7010-TT3651 DCB specimens

Number of days

nr.	nominal crack length (mm)	Number of days																						
		2	6	9	13	16	22	30	37	44	51	57	65	71	85	100	114	127	141	155	169	183	196	
LN 65666																								
A1.1	25	-	-	-	-	-	-	-	-	-	-	-	-	-	-	-	-	-	-	-	-	-	-	-
A2.3	25	-	-	-	-	-	-	-	-	-	-	-	-	-	-	-	-	-	-	-	-	-	-	-
A3.1	25	-	-	-	-	-	-	-	-	-	-	-	-	-	-	-	-	-	-	-	-	-	-	-
A1.9	40	-	-	-	-	-	-	-	-	-	-	-	-	-	-	-	-	-	-	-	-	-	-	-
A2.11	40	-	-	-	-	-	-	-	-	-	-	-	-	-	-	-	-	-	-	-	-	-	-	-
A3.9	40	-	-	-	-	-	-	-	-	-	-	-	-	-	-	-	-	-	-	-	-	-	-	-
B1.1	25	-	-	-	-	-	-	-	-	-	-	-	-	-	-	-	-	-	-	-	-	-	-	-
B2.1	25	-	-	-	-	-	-	-	-	-	-	-	-	-	-	-	-	-	-	-	-	-	-	-
B3.1	25	-	-	-	-	-	-	-	-	-	-	-	-	-	-	-	-	-	-	-	-	-	-	-
B1.9	40	-	-	-	-	-	-	-	-	-	-	-	-	-	-	-	-	-	-	-	-	-	-	-
B2.9	40	-	-	-	-	-	-	-	-	-	-	-	-	-	-	-	-	-	-	-	-	-	-	-
B3.9	40	-	-	-	-	-	-	-	-	-	-	-	-	-	-	-	-	-	-	-	-	-	-	-
NaCl moistening																								
B1.1	25	-	-	-	-	-	-	-	-	-	-	-	-	-	-	-	-	-	-	-	-	-	-	-
B2.1	25	-	-	-	-	-	-	-	-	-	-	-	-	-	-	-	-	-	-	-	-	-	-	-
B3.1	25	-	-	-	-	-	-	-	-	-	-	-	-	-	-	-	-	-	-	-	-	-	-	-
B1.9	40	-	-	-	-	-	-	-	-	-	-	-	-	-	-	-	-	-	-	-	-	-	-	-
B2.9	40	-	-	-	-	-	-	-	-	-	-	-	-	-	-	-	-	-	-	-	-	-	-	-
B3.9	40	-	-	-	-	-	-	-	-	-	-	-	-	-	-	-	-	-	-	-	-	-	-	-
LN 65666																								
A1.2	25	-	-	-	-	-	-	-	-	-	-	-	-	-	-	-	-	-	-	-	-	-	-	-
A2.6	25	-	-	-	-	-	-	-	-	-	-	-	-	-	-	-	-	-	-	-	-	-	-	-
A3.2	25	-	-	-	-	-	-	-	-	-	-	-	-	-	-	-	-	-	-	-	-	-	-	-
A1.10	40	-	-	-	-	-	-	-	-	-	-	-	-	-	-	-	-	-	-	-	-	-	-	-
A2.12	40	-	-	-	-	-	-	-	-	-	-	-	-	-	-	-	-	-	-	-	-	-	-	-
A3.10	40	-	-	-	-	-	-	-	-	-	-	-	-	-	-	-	-	-	-	-	-	-	-	-
B1.2	25	-	-	-	-	-	-	-	-	-	-	-	-	-	-	-	-	-	-	-	-	-	-	-
B2.3	25	-	-	-	-	-	-	-	-	-	-	-	-	-	-	-	-	-	-	-	-	-	-	-
B3.2	25	-	-	-	-	-	-	-	-	-	-	-	-	-	-	-	-	-	-	-	-	-	-	-
B1.10	40	-	-	-	-	-	-	-	-	-	-	-	-	-	-	-	-	-	-	-	-	-	-	-
B2.10	40	-	-	-	-	-	-	-	-	-	-	-	-	-	-	-	-	-	-	-	-	-	-	-
B3.10	40	-	-	-	-	-	-	-	-	-	-	-	-	-	-	-	-	-	-	-	-	-	-	-

A = 7010-TT651
 B = 7010-TT3651
 L crack growth in mm

TABLE 8
Stress corrosion crack growth measurements

specimen nr.	mean crack growth* measured from the fracture surface (mm)	crack growth measured from specimen side (mm)	percentage of initial prescribed displacement which is left after unloading the specimens
A1.1	4.35	2.8	61
A2.3	2.1	0.4	42
A3.1	4.3	3.2	40
A1.9	4.4	3.75	40
A2.11	1.9	1.35	28
A3.9	3.6	2.	39
B1.1	1.85	0.35	49
B2.1	1.5	0.25	34
B3.1	1.9	0.2	47
B1.9	1.9	1.	34
B2.9	0.7	0.25	30
B3.9	1.6	0.35	31
A1.2	1.0	0.05	10
A2.6	-	0.05	3
A3.2	-	-	8
A1.10	1.2	0.25	5
A2.12	-	-	4
A3.10	0.4	0.1	-
B1.2	0.4	-	5
B2.3	-	0.1	4
B3.2	-	0.5	5
B1.10	0.3	0.1	5
B2.10	-	0.1	7
B3.10	-	0.05	22

* mean value of the crack lengths at $\frac{1}{4}$, $\frac{1}{2}$ and $\frac{3}{4}$ of the specimen thickness

TABLE 9a
Experimental results for compact tension tests

specimen	a mm	P _Q kN	K _Q MPa m ^{3/2}	σ _{0.2} MPa	2.5($\frac{K_Q}{\sigma_{0.2}}$) mm	K _Q mean MPa m ^{3/2}	$\frac{P_{max}}{P_Q}$	$\frac{K_{f max}}{K_Q}$	* does not obey ASTM reg. nr.
ALS1	20.1	17.38	41.9	474	19.5	41.5	1.10	0.39	8
ALS2	19.5	17.80	41.1	474	18.8		1.20	0.39	5;8
ALT1	18.6	15.29	33.1	474	12.2	33.5	1.04	0.42	**
ALT2	18.0	16.27	33.9	474	12.8		1.00	0.39	**
ATS1	17.8	15.33	31.5	469	11.3	31.6	1.07	0.45	8
ATS2	17.9	15.36	31.7	469	11.4		1.06	0.45	**
ATL1	18.4	14.65	31.4	469	11.2	30.4	1.00	0.37	**
ATL2	18.9	13.24	29.3	469	9.8		1.01	0.41	**
AST1	18.6	12.47	27.0	414	10.6	27.1	1.03	0.51	6
AST2	17.9	13.08	27.1	414	10.7		1.00	0.49	**
ASL1	19.2	12.14	27.5	414	11.0	27.2	1.00	0.44	**
ASL2	18.6	12.41	26.9	414	10.6		1.00	0.43	**
BLS1	19.1	19.02	42.8	436	24.1	43.1	1.20	0.36	1;2;5;8
BLS2	19.0	19.41	43.3	436	24.7		1.15	0.35	1;2;5;8
BLT1	18.0	17.69	36.8	436	17.8	36.5	1.00	0.36	**
BLT2	17.5	17.97	36.2	436	17.2		1.05	0.35	3
BTS1	18.6	16.06	34.8	432	16.2	35.2	1.09	0.43	**
BTS2	18.7	16.27	35.5	432	16.9		1.05	0.42	**
BTL1	18.5	14.87	32.1	432	13.8	32.5	1.01	0.36	**
BTL2	18.8	14.97	32.9	432	14.5		1.00	0.36	**
BST1	17.9	14.15	29.3	384	14.6	29.0	1.00	0.45	**
BST2	18.4	13.36	28.6	384	1.39		1.04	0.48	**
BSL1	18.9	13.06	28.9	384	14.2	29.7	1.02	0.41	**
BSL2	18.7	13.96	30.5	384	15.8		1.00	0.39	**
CLS1	18.8	22.44	49.3	429	33.0	47.8	1.29	0.31	1;2;5;8
CLS2	18.9	20.96	46.3	429	29.1		1.33	0.33	1;2;5;8
CLT1	18.6	20.55	44.5	429	26.9	43.3	1.07	0.31	1;2
CLT2	19.6	10.11	42.1	429	24.1		1.09	0.35	1;2
CTS1	19.0	19.22	42.9	427	25.2	41.9	1.10	0.36	1;2;8
CTS2	19.0	18.39	40.9	427	22.9		1.14	0.37	1;2;5;8
CTL1	18.8	18.20	40.1	427	22.0	39.9	1.01	0.30	1;2
CTL2	18.7	18.16	39.6	427	21.5		1.03	0.30	1;2
CTS1	18.5	15.44	33.2	380	19.1	34.1	1.10	0.41	2
CTS2	19.8	14.86	35.0	380	21.2		1.02	0.43	1;2
CSL1	19.6	14.38	33.5	380	19.4	34.4	1.04	0.38	**
CSL2	19.5	15.21	35.2	380	21.5		1.02	0.35	1

A = 7010-T7651
B = 7010-T73651
C = 7010-T7351

* See appendix A
** valid K_{Ic}

TABLE 9b

Experimental results for SENB specimens

specimen	a mm	P _Q kN	K _Q MPa m ^{1/2}	σ _{0.2} MPa	2.5($\frac{K_Q}{\sigma_{0.2}}$) mm	K _Q mean MPa m ^{1/2}	$\frac{P_{max}}{P_Q}$	$\frac{K_{f max}}{K_Q}$	does not obey ASTM reg. nr. in Appendix A
ATS1	18.6	15.06	31.4	469	11.2	31.7	1.03	0.42	
ATS2	19.6	14.18	32.0	469	11.6		1.03	0.49	7
BTS1	19.4	15.28	33.9	432	15.4	34.0	1.14	0.46	5
BTS2	19.7	14.93	34.0	432	15.5		1.08	0.47	
CTS1	19.1	16.98	36.9	427	18.7	37.6	1.20	0.41	5
CTS2	19.1	17.57	38.2	427	20.0		1.19	0.40	2;5

TABLE 10

Position of severest flights in the standardized sequence

Flight type	A	B	C	D
Flight No. in sequence	1656	2856	501	106
			2936	412
			3841	684
				1099
				1653
				2682
				3360
				3538
				3898

TABLE 11

Definition of flight types and number of load cycles within each flight

Flight type	Number of flights in one block of 4,000 flights	Number of gust loads (full cycles) at the 10 amplitude levels										Total number of cycles per flight
		I	II	III	IV	V	VI	VII	VIII	IX	X	
A	1	1	1	1	4	8	18	64	112	391	900	1500
B	1		1	1	2	5	11	39	76	366	899	1400
C	3			1	1	2	7	22	61	277	879	1250
D	9				1	1	2	14	44	208	680	950
E	24					1	1	6	24	165	603	800
F	60						1	3	19	115	512	650
G	181							1	7	70	412	490
H	420								1	16	233	250
I	1090									1	69	70
J	2211										25	25
Total number of cycles per block of 4,000 flights		1	2	5	18	52	152	800	4.170	34.800	358.665	
Cumulative number of load cycles per block of 4,000 flights		1	3	8	26	78	230	1.030	5.200	40.000	398.665	

TABLE 12
Survey of fatigue crack growth lives

alloy	thickness mm	Surface		Centre		Surface		Mean	
		N _f	li	N _f	li	N _f	li	N _f	li
7010T7651	2	5626*	6.7	6857	6.6	6575	7.0	6716	6.8
	5	4924	6.8	6071	6.9	4889	6.9	4961	6.9
	10	4429	7.3	4241	7.3	4501	7.3	4391	7.3
	15	2858**	8.3	3695	7.1	5099**		3695	7.1
7010T73651	2	6937	6.8	6898	7.0	7428***	6.15	7088	6.7
	5	5465	6.75	5379	6.9	5404	6.75	5416	6.8
	10	4960	6.5	4684	7.1	5032	7.0	4892	6.9
	15	4503	7.2	4505	6.8	4414	7.4	4474	7.1
7075T7351	5	5654	6.9	5461	6.9	5633	7.0	5583	6.9
	10	4685	7.0	4832	7.1	4814	7.2	4777	7.1
	15	5382	6.3	4738	6.6	4819	7.0	4980	6.6

N_f = total fatigue life in flights

li = mean initial crack length in mm.

* unreliable result

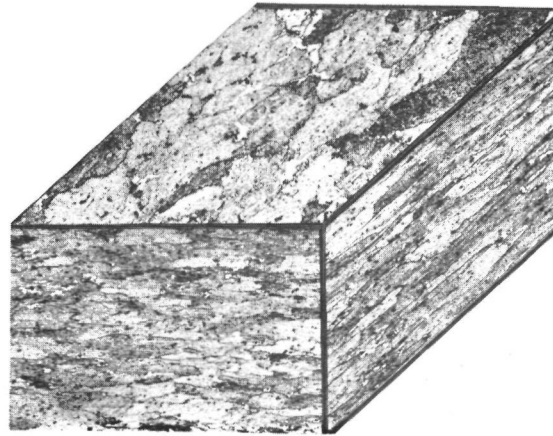
** front of precrack very asymmetric

*** fatigue test started at flight nr. 2936 instead of flight nr. 1

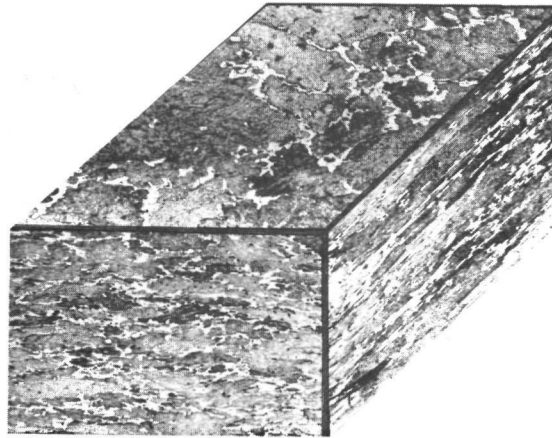
TABLE 13

Number of flights for crack growth from 10 to 20 mm

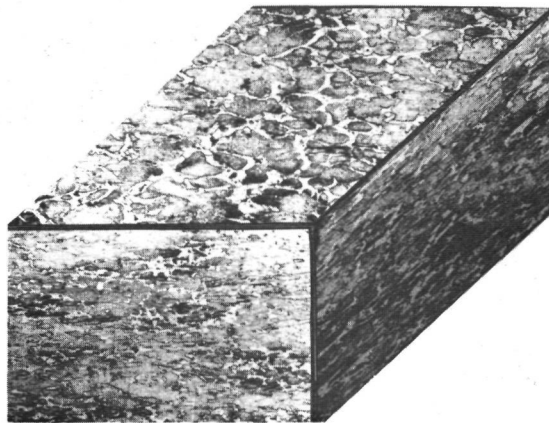
alloy	thickness (mm)	N ₁₀₋₂₀		
		surface	centre	surface
7010-T7651	2	-	2390	2540
	5	1760	1840	1785
	10	1600	1670	1590
	15	1680	1585	1670
7010-T73651	2	2870	2880	2740
	5	2200	2160	2105
	10	1820	1635	1795
	15	1660	1885	1450
7075-T7351	5	2230	2320	2370
	10	1770	1980	1910
	15	1840	1725	1930



SURFACE

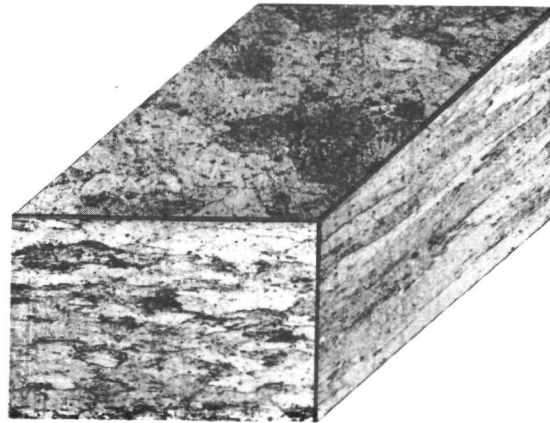


$\frac{1}{4}t$

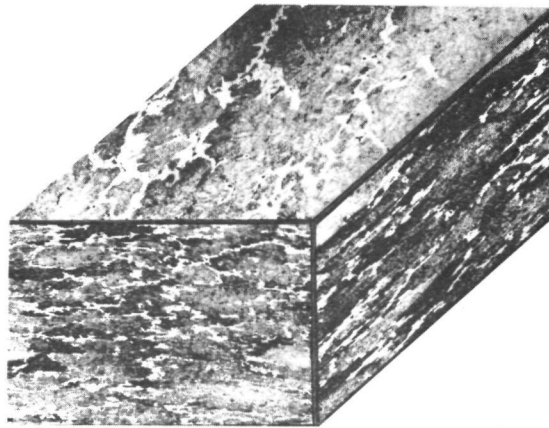


$\frac{1}{2}t$

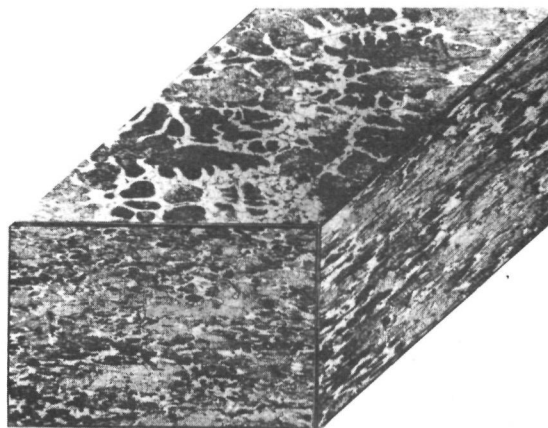
Fig. 1 Grain orientations in 7010-T7651 (x 17.2)



SURFACE

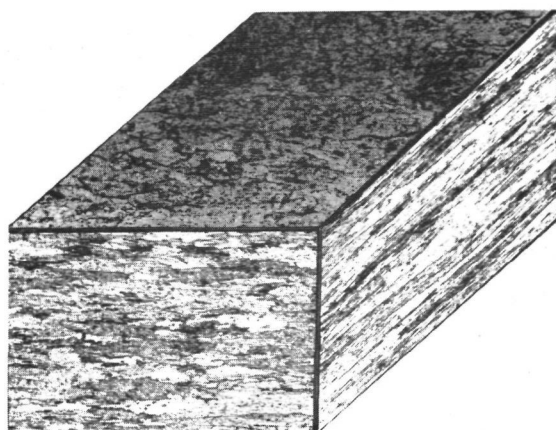


$\frac{1}{4}t$

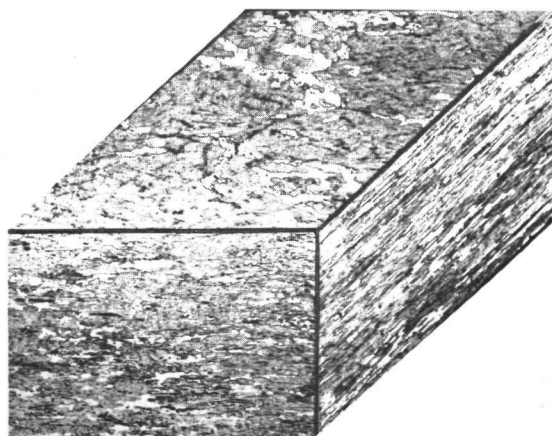


$\frac{1}{2}t$

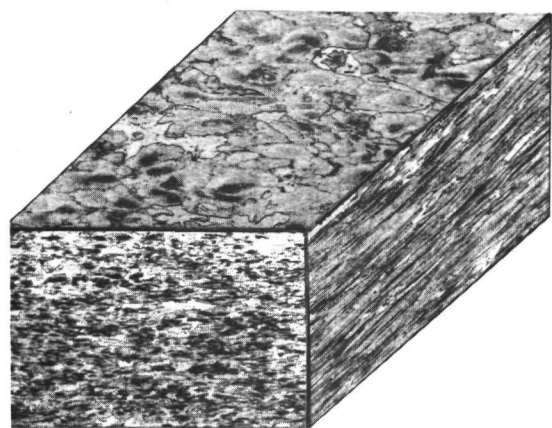
Fig. 2 Grain orientations in 7010-T73651 (x 17.2)



SURFACE



$\frac{1}{4}t$



$\frac{1}{2}t$

Fig. 3 Grain orientations in 7075-T7351 (x 17.2)

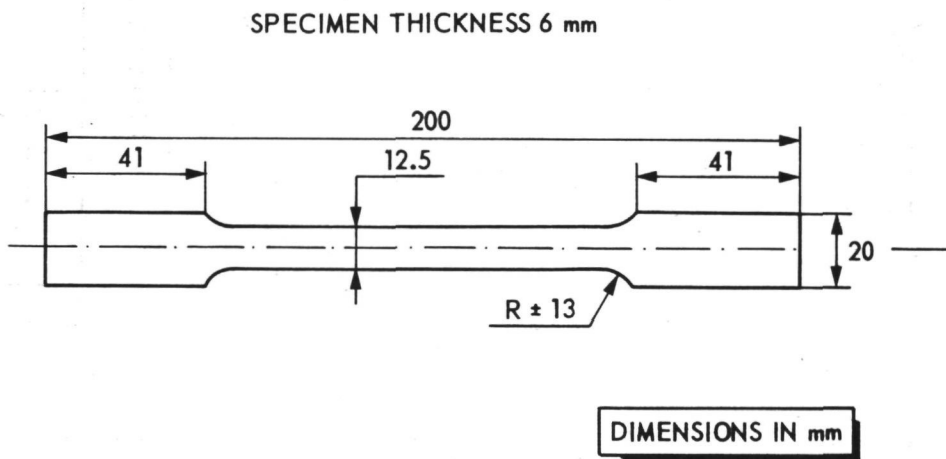


Fig. 4 Rectangular tensile test specimen conforming to ASTM specification E8-69

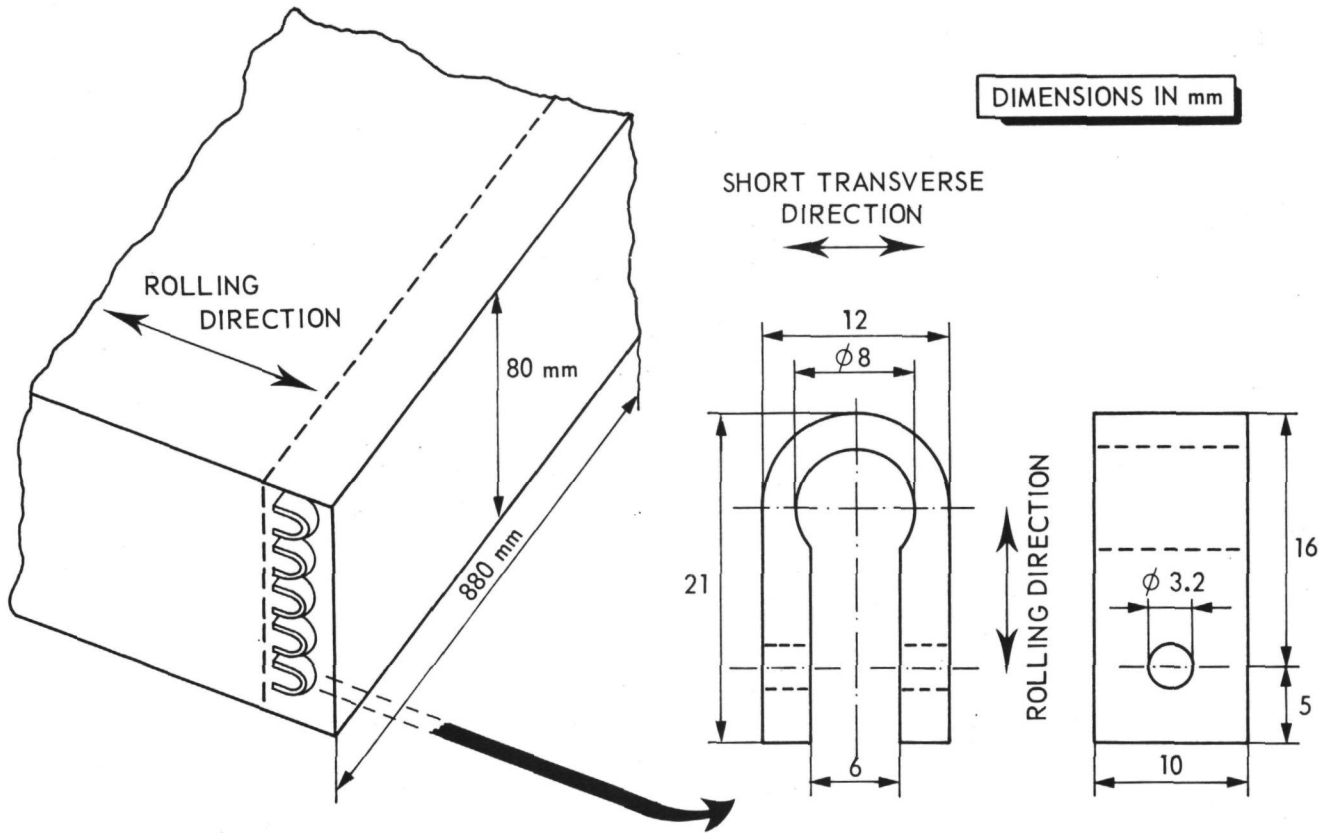


Fig. 5 Location and dimensions of the stress corrosion crack initiation specimens

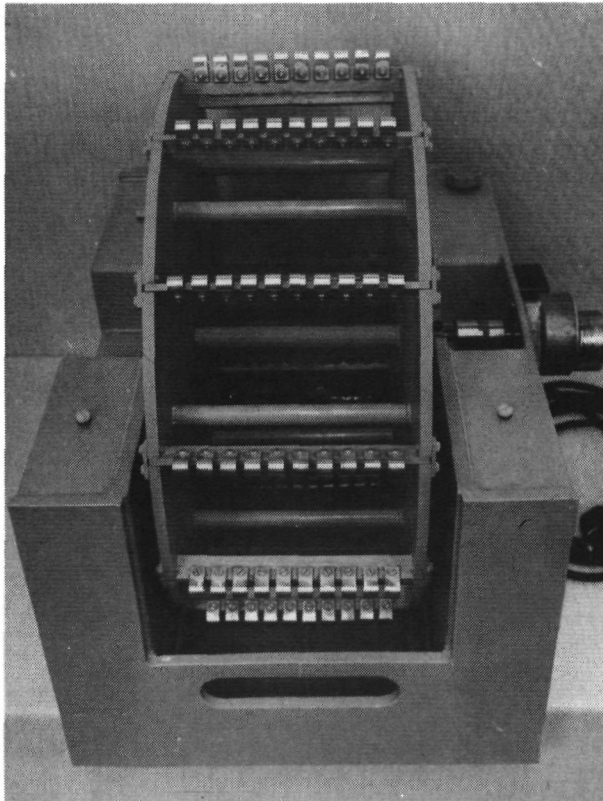


Fig. 6 Paddle wheel, used for stress corrosion crack initiation tests

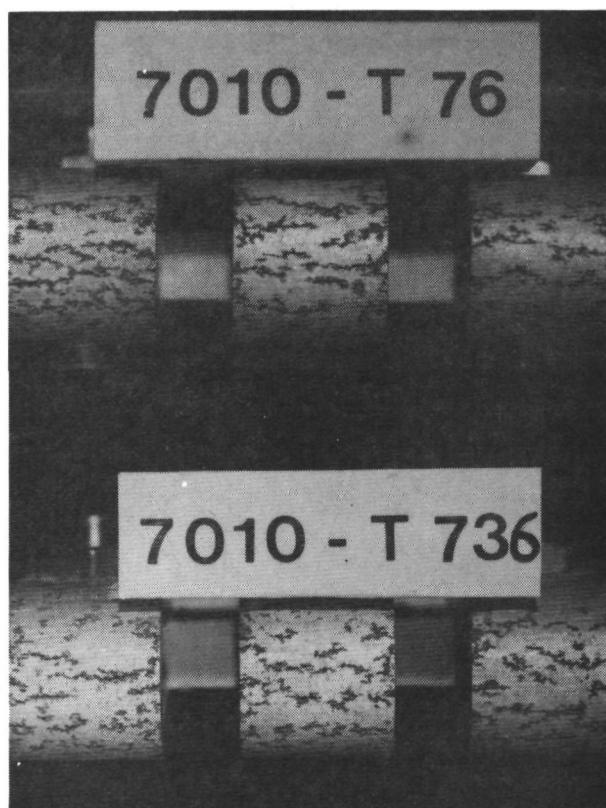


Fig. 7 Corrosive attack of 7010-T7651 and 7010-T73651 after 1400 hours of testing by alternate immersion

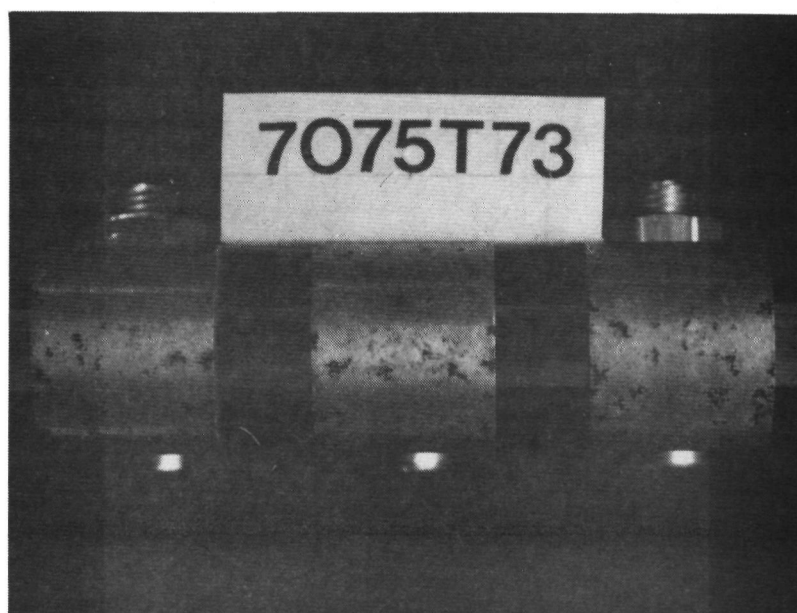


Fig. 8 Corrosive attack of 7075-T7351 specimens after 1400 hours of testing by alternate immersion

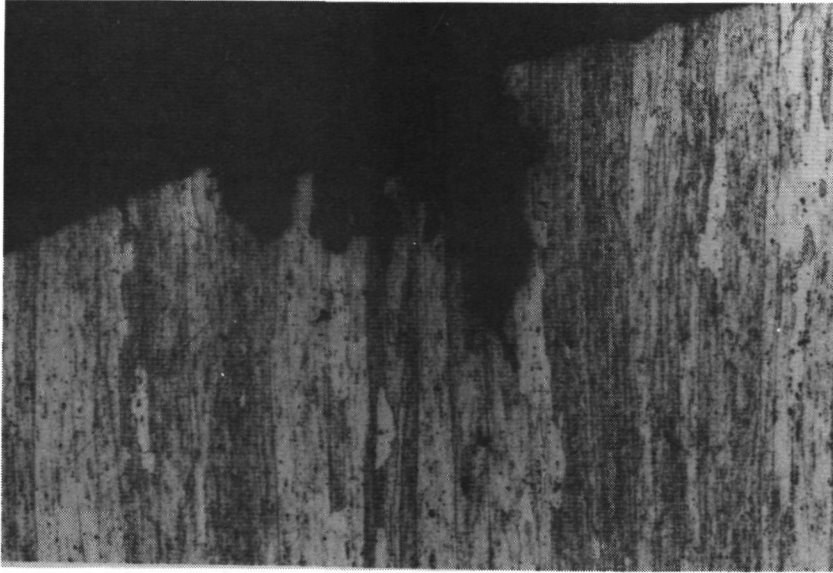


Fig. 9 Corrosion pit in a 7075-T7351 specimen after alternate immersion (x 65.3)

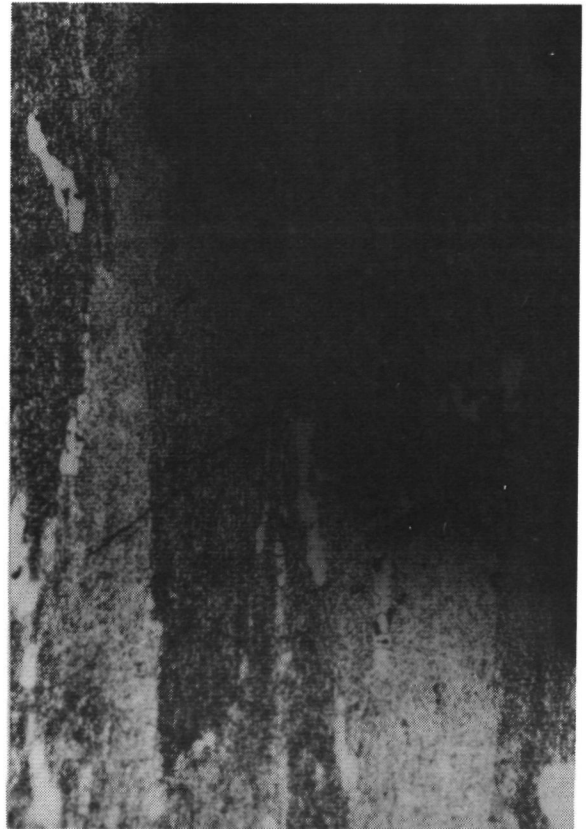


Fig. 10 Corrosion pits in 7010-T73651 specimens and transgranular cracks emanating from the corrosion pits (x 144)

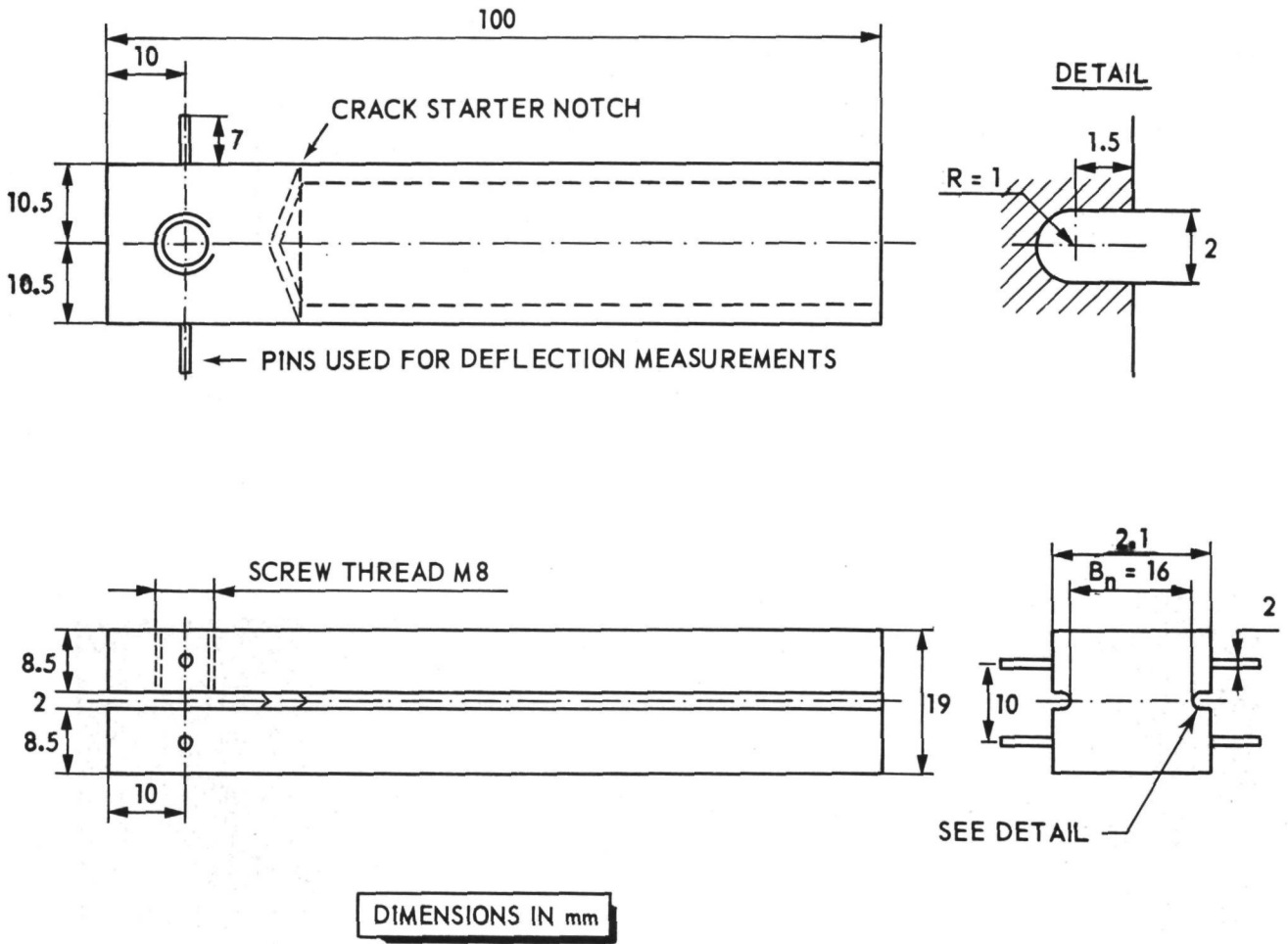


Fig. 11 Double Cantilever Beam (DCB) test specimen

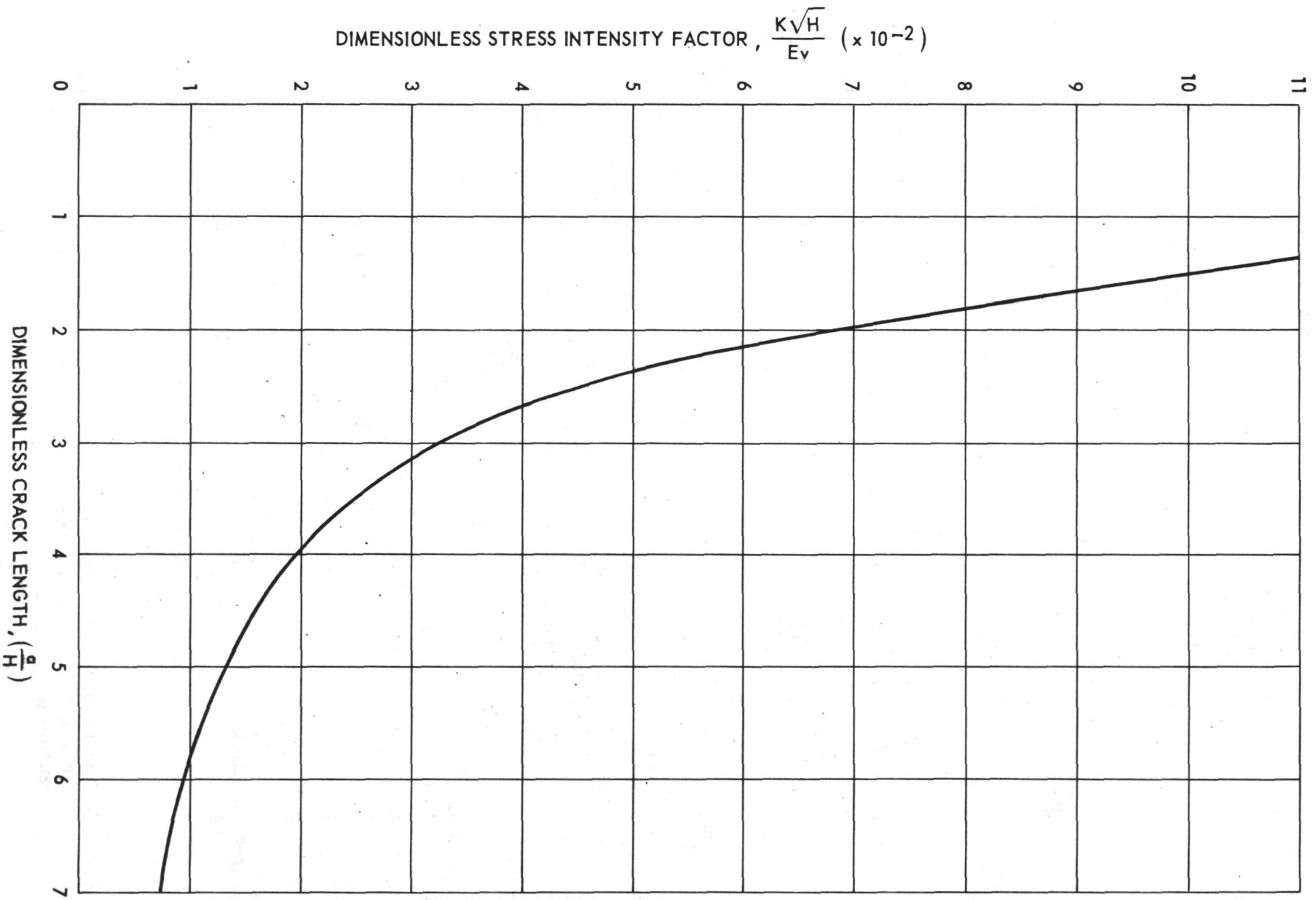


Fig. 12 The K-calibration curve as a function of crack length (Ref.5)

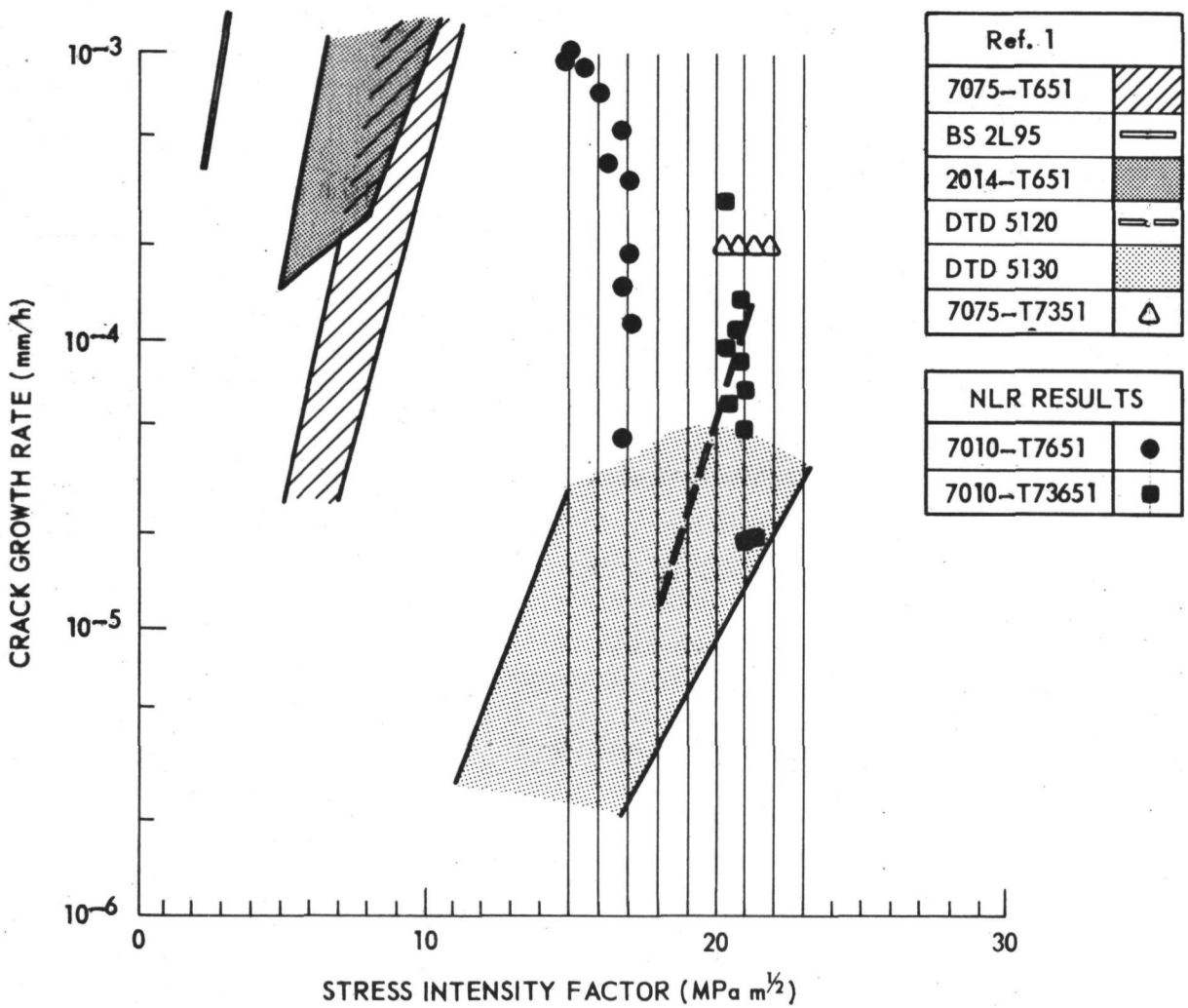
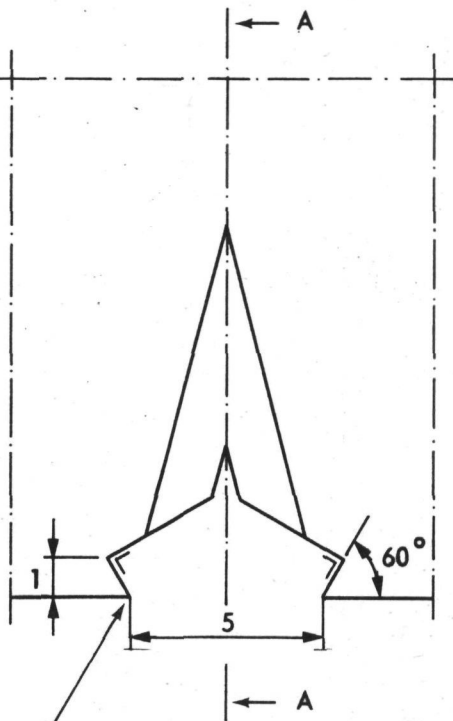
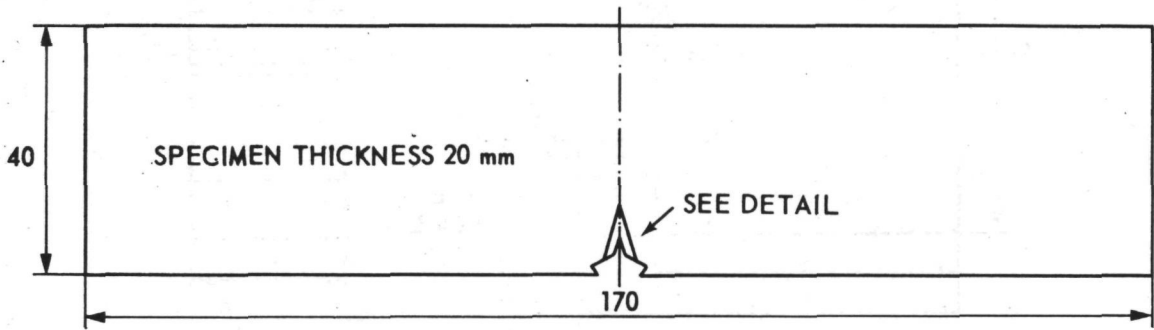
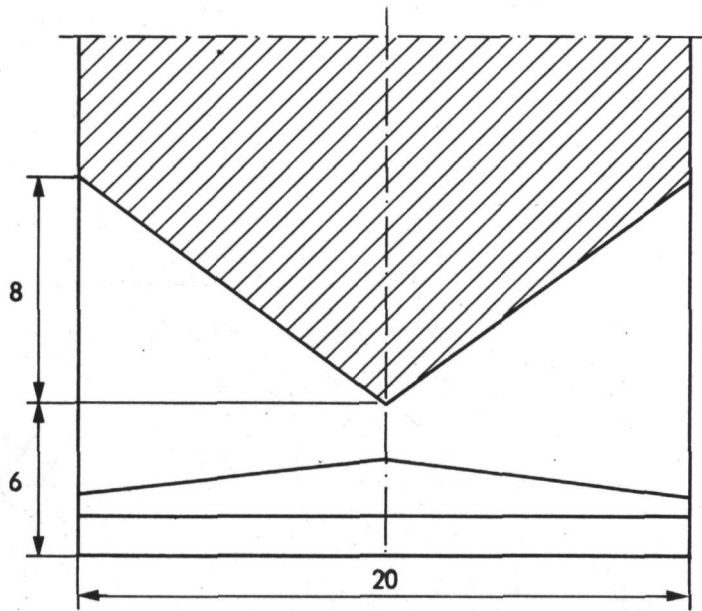


Fig. 13 The stress corrosion crack growth rates for DCB specimens tested in the S-L direction and moistened twice daily with a sodium chloride solution.



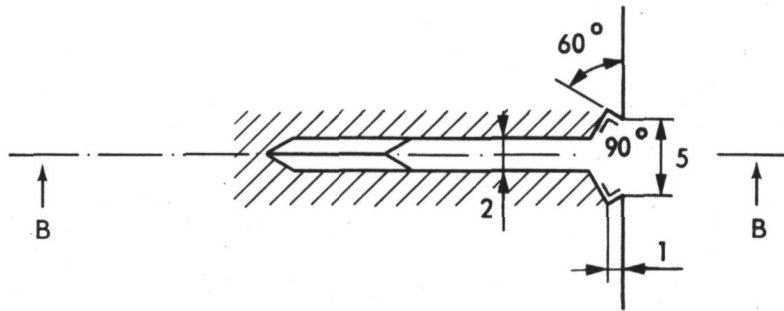
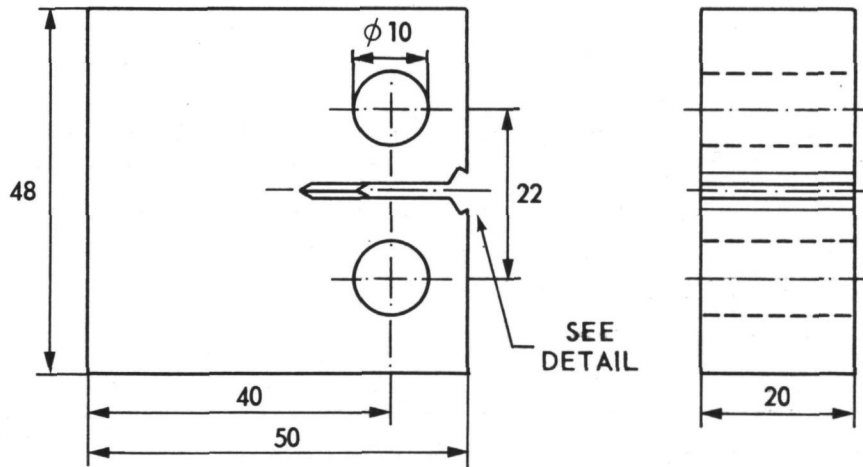
SEATING FOR CLIP GAUGE



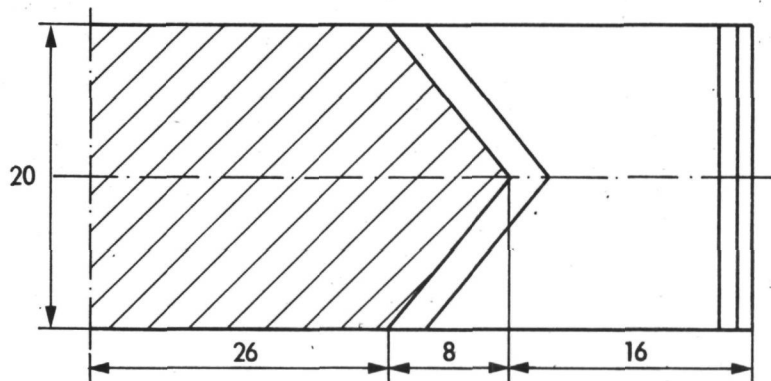
SECTION A - A

DIMENSIONS IN mm

Fig. 14 Fracture toughness specimen of the type: Single Edge Notch Bend (SENB)



DETAIL NOTCH



SECTION B-B

DIMENSIONS IN mm

Fig. 15 Fracture toughness specimen of the type: Compact Tension (CT)

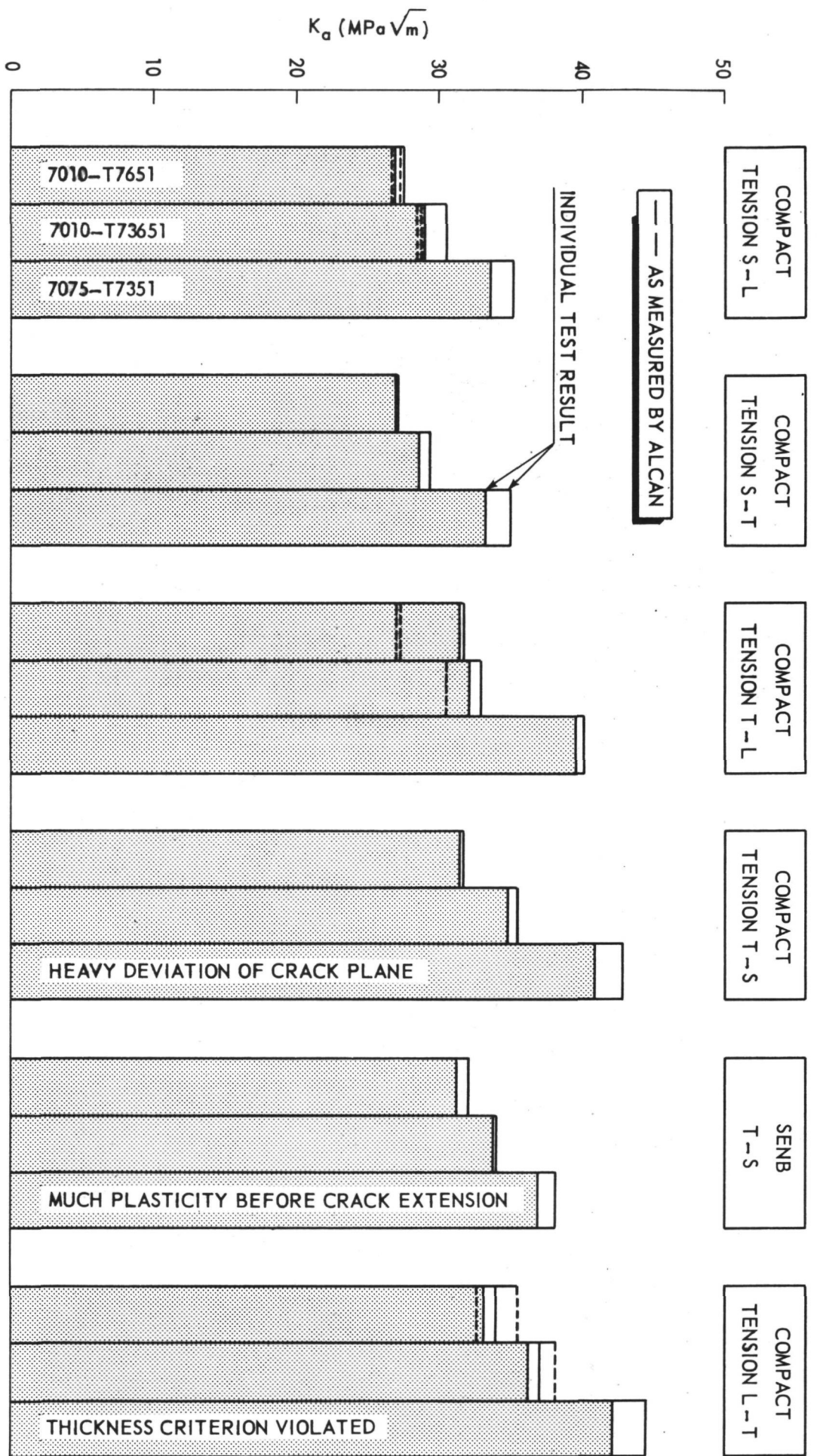


Fig. 16 Fracture toughness properties for various test orientations

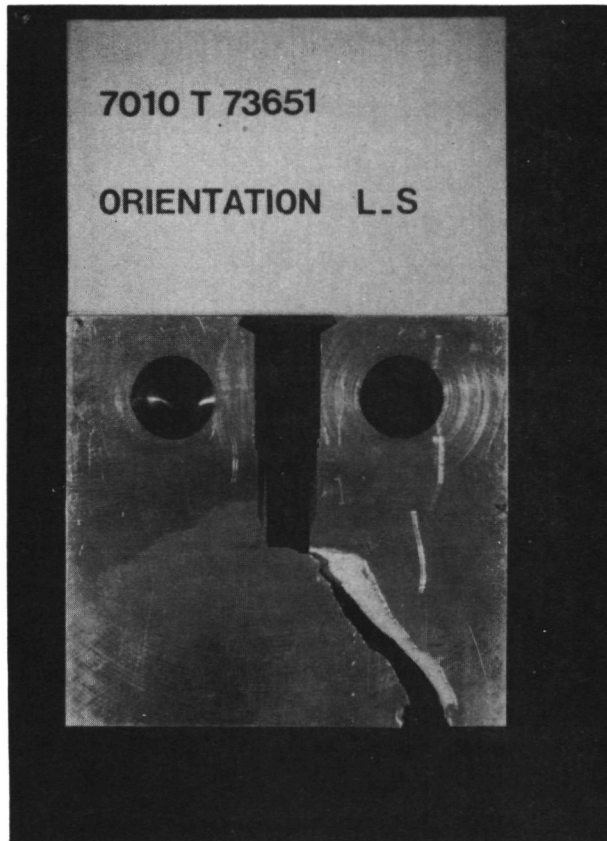


Fig. 17 Declination of the crack plane from the short transverse direction

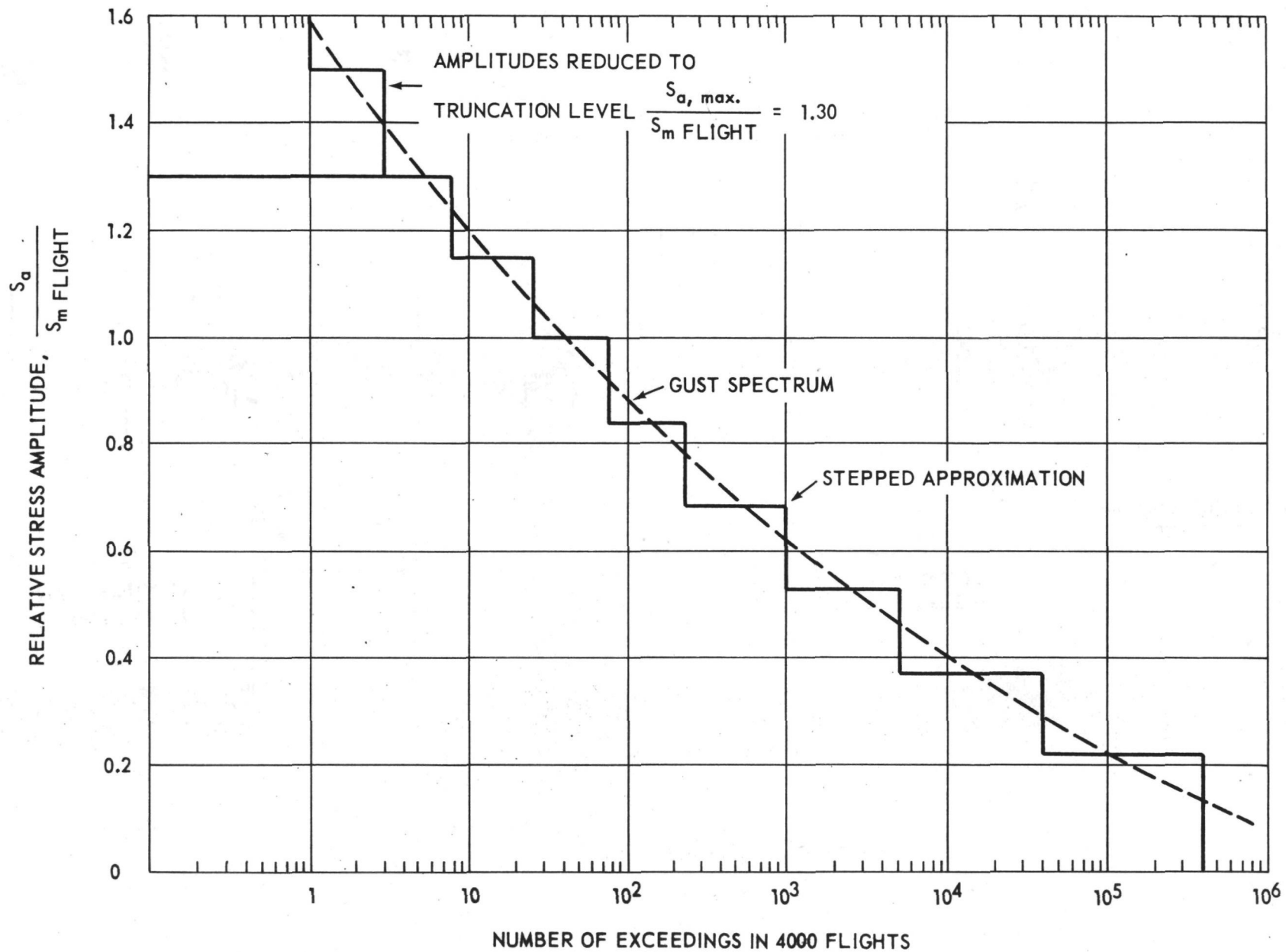


Fig. 18 The gust load spectrum

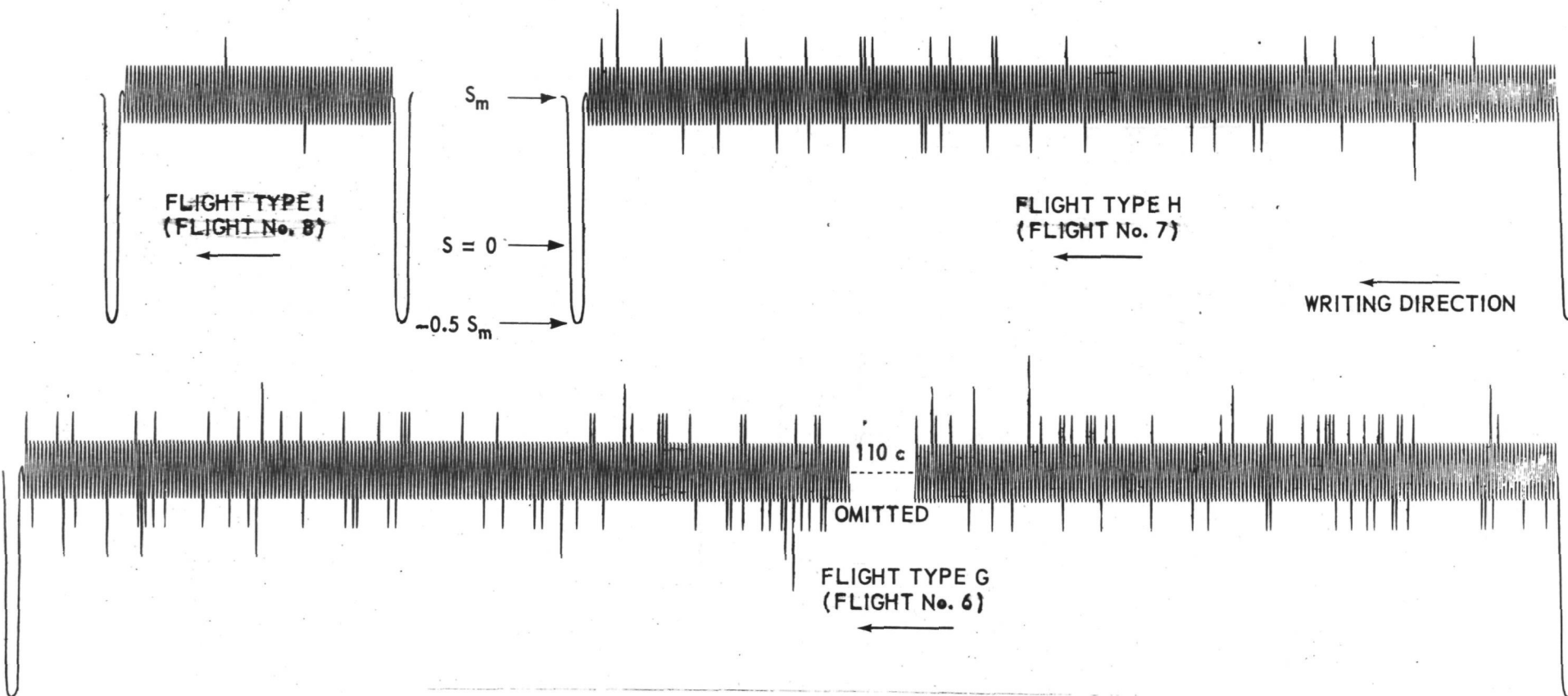


Fig. 19 Examples of different flight types

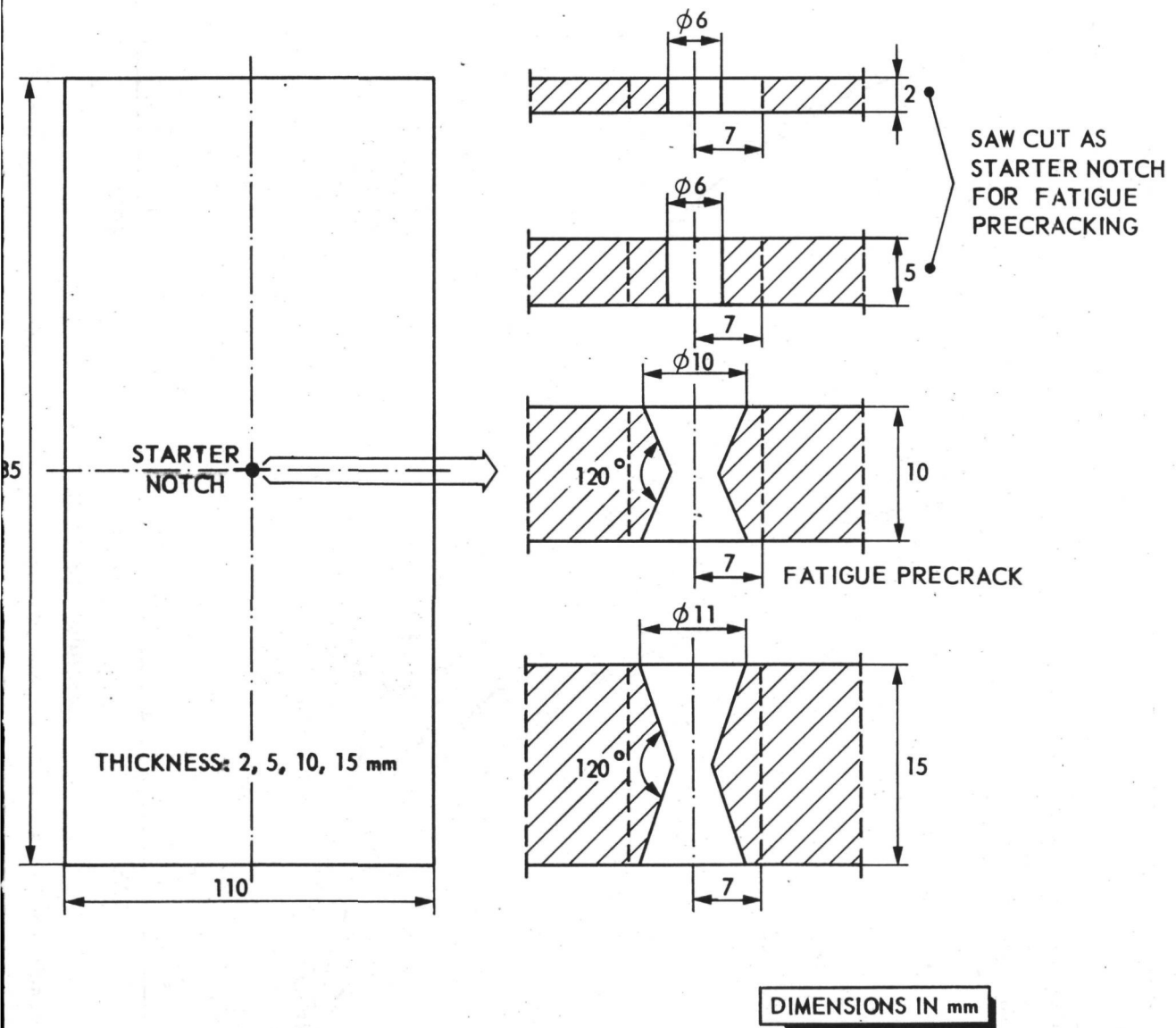


Fig. 20 Dimensions of fatigue specimen

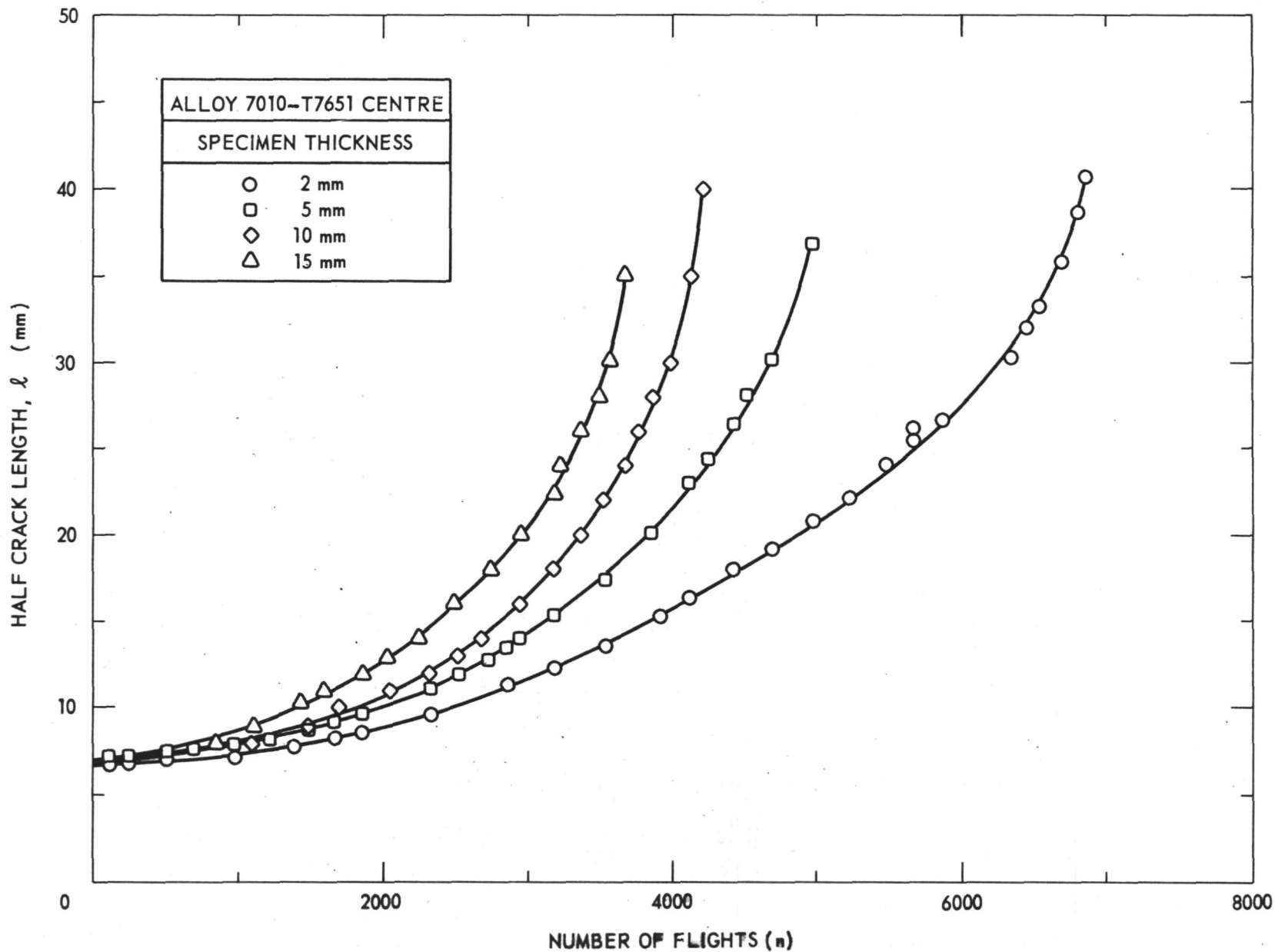


Fig. 21 Half crack length as a function of the number of flights for different specimen thicknesses.

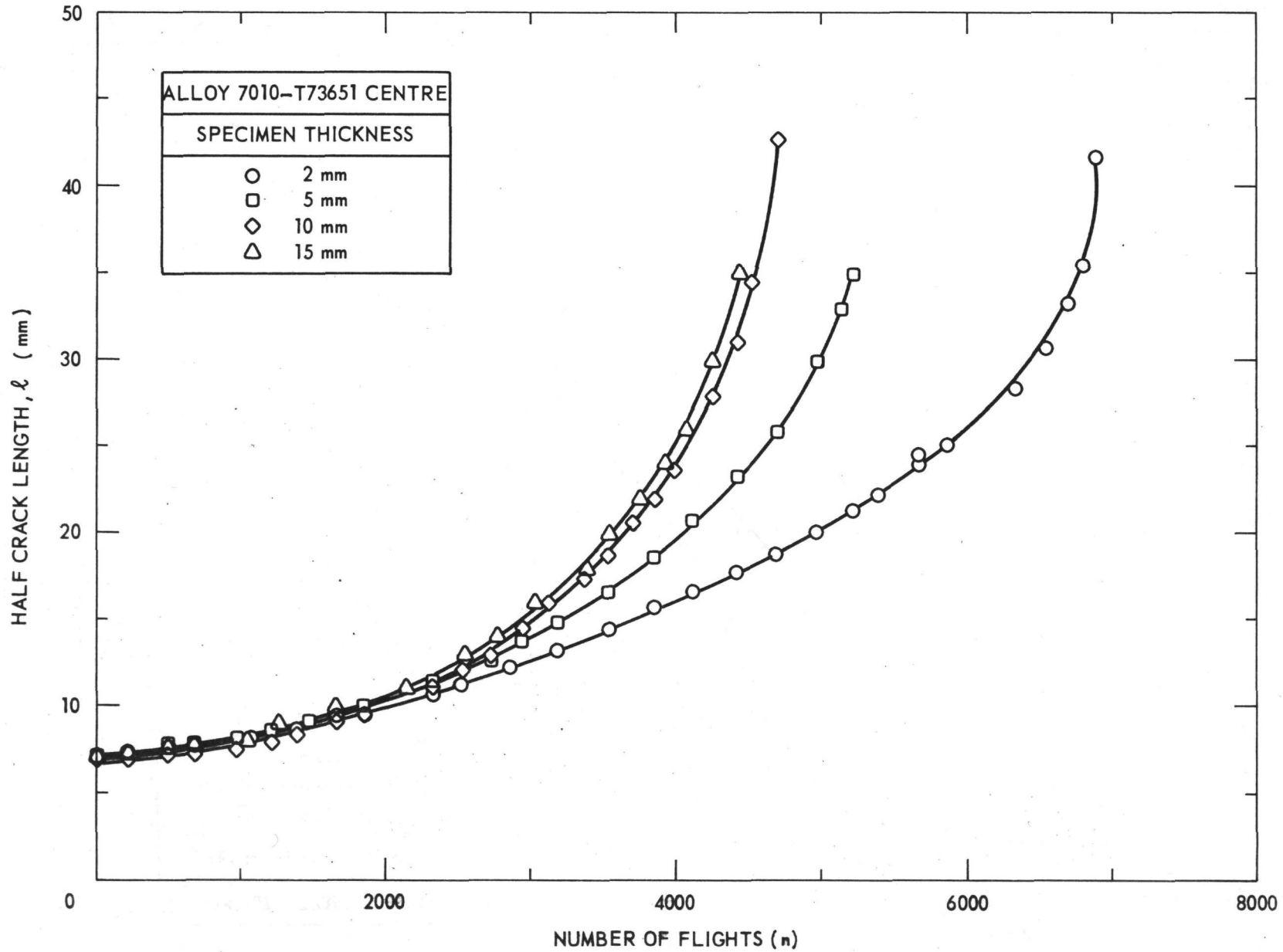


Fig. 22 Half crack length as a function of the number of flights for different specimen thicknesses

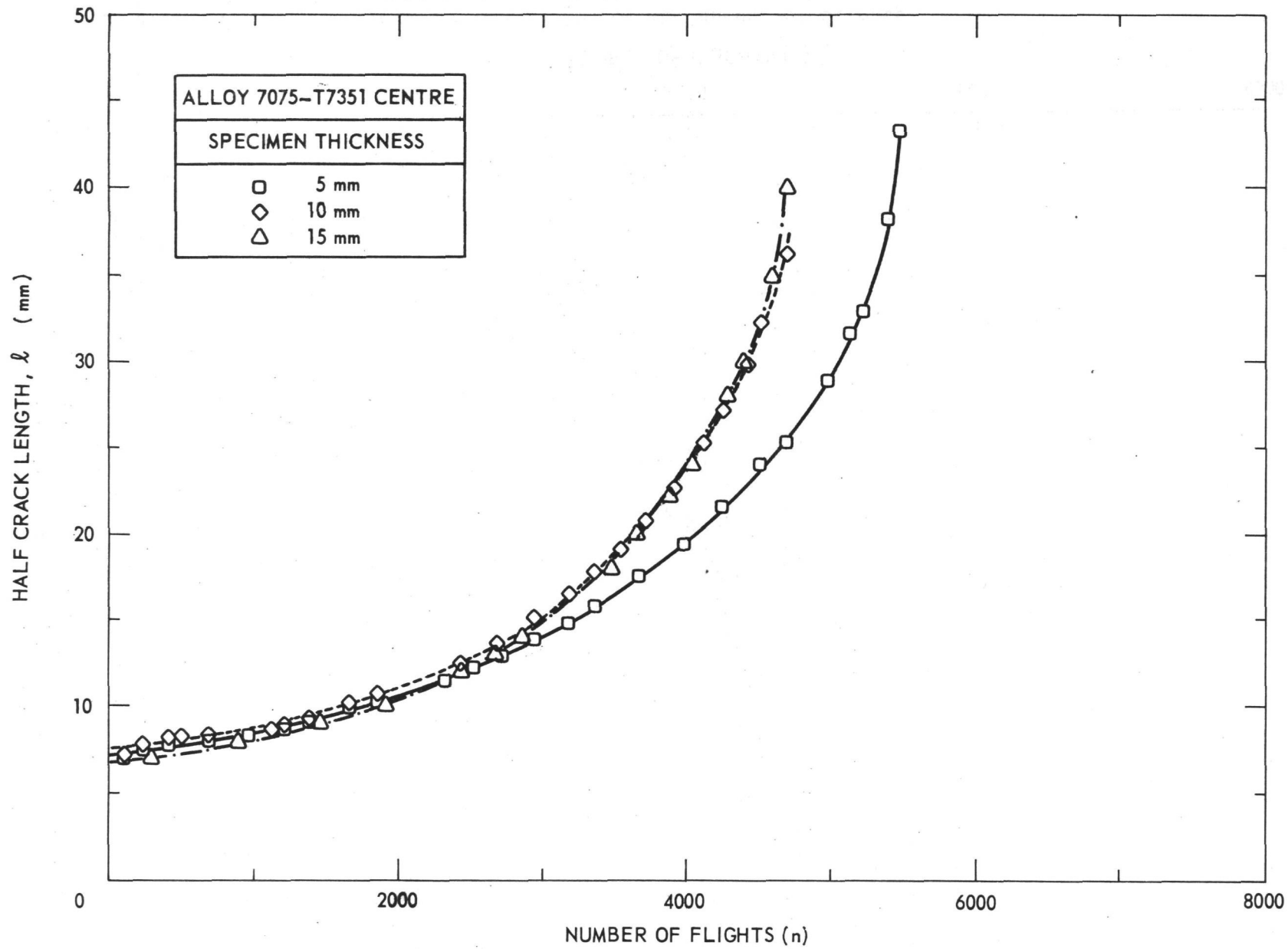


Fig. 23 Half crack length as a function of the number of flights for different specimen thicknesses

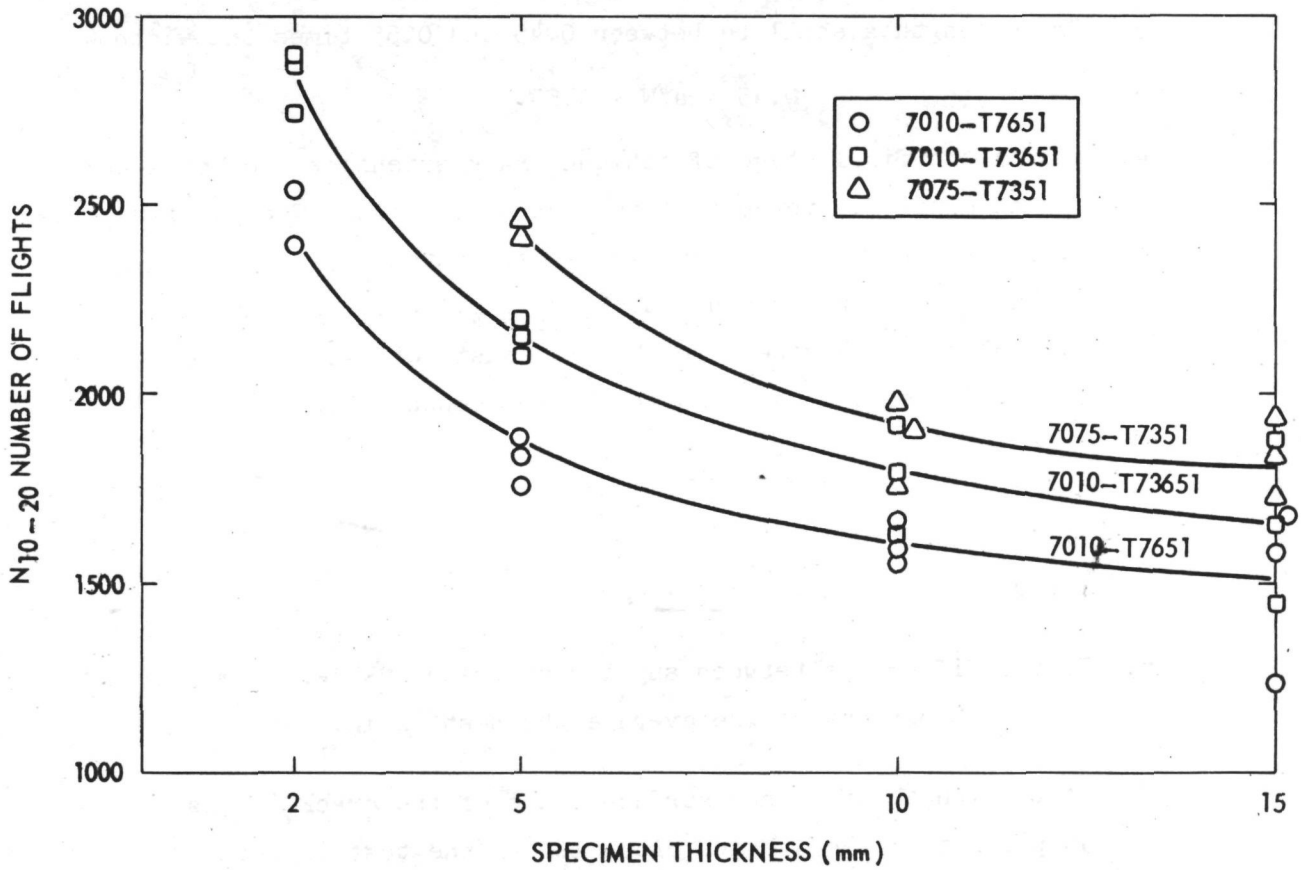


Fig. 24 Influence of the sheet thickness on fatigue crack growth

APPENDIX A REQUIREMENTS FOR FRACTURE TOUGHNESS TESTING

1. Specimen thickness B shall exceed $2.5 \left(\frac{K_{Ic}}{\sigma_{ys}} \right)^2$
2. Crack length a shall exceed $2.5 \left(\frac{K_{Ic}}{\sigma_{ys}} \right)^2$
3. Crack length a shall be between 0.45 and 0.55 times the width W
$$0.45 < a/W < 0.55$$
4. During the final stage of fatigue crack extension, for at least the terminal 2.5 percent of the over-all length of notch plus crack, the ratio of the maximum stress intensity of the fatigue cycle to the Young's modulus, $K_{f(max)}/E$, shall not exceed $0.00032 \text{ m}^{1/2}$. Furthermore, $K_{f(max)}$ must not exceed 60 percent of the K_Q value determined in the subsequent test

$$\left(\frac{K_{f(max)}}{K_Q} \right) < 0.6$$

5. The ratio $\frac{P_{max}}{P_Q}$ shall not exceed 1.10
6. If the difference between any two of the crack length measurements exceeds 5 percent of the average the test is invalid
7. If the length of either surface trace of the crack is less than 90 percent of the average crack length the test is invalid.
8. The crack plane shall be parallel to both the specimen width and thickness directions within ± 10 deg.

